Materials Horizons

ROYAL SOCIETY OF CHEMISTRY

REVIEW

View Article Online
View Journal

Cite this: DOI: 10.1039/d6mh00433d

Soft robotic cardiac sleeves: materials, actuation mechanisms and translational pathways

Javad Foroughi, *[ae] Sinmisola Aloko,[a] Geoffrey Spinks,[b] Liao Wu,[a] Shuying Wu,[c] Christopher Hayward,[d] Chun H. Wang[a] and Arjang Ruhparwar[e]

Heart failure remains a leading cause of morbidity and mortality worldwide, highlighting the urgent need for effective alternatives to heart transplantation. While ventricular assist devices (VADs) have improved survival for patients with advanced heart failure, their long-term use is associated with blood-contact complications, thromboembolic risk, and the need for lifelong anticoagulation. These limitations have stimulated interest in non-blood-contact mechanical circulatory support strategies, particularly devices based on direct cardiac compression (DCC). Recent advances in soft robotics, compliant materials, and bioinspired actuation technologies have enabled the development of soft robotic cardiac sleeves that assist cardiac function by mechanically compressing the heart in synchrony with native myocardial contraction. By avoiding direct blood interaction, these systems aim to reduce thrombogenic risks while preserving physiological cardiac mechanics. This review provides an overview of emerging soft robotic cardiac compression devices, focusing on the materials, actuation mechanisms, and design strategies that enable effective epicardial assistance. Key engineering challenges, including conformal heart–device coupling, cyclic durability, and synchronisation with cardiac dynamics, are discussed. Finally, we outline translational considerations and future research directions required to advance these technologies toward clinical application.

Received 9th March 2026,
Accepted 8th April 2026

DOI: 10.1039/d6mh00433d

rsc.li/materials-horizons

Wider impact

Heart failure remains one of the most significant global health challenges, affecting more than 60 million people worldwide and placing enormous strain on healthcare systems. Current mechanical circulatory support technologies primarily rely on blood-contacting ventricular assist devices, which are associated with thrombosis, infection, and the need for lifelong anticoagulation. Advances in soft materials, artificial muscles, and bioinspired actuation now provide new opportunities to develop non-blood-contact cardiac assist technologies based on direct cardiac compression. This review highlights how emerging materials systems, including soft elastomers, electroactive polymers, dielectric elastomers, and twisted-and-coiled polymer muscles, are enabling a new class of biointegrated soft robotic devices capable of replicating physiological cardiac mechanics. Beyond cardiac therapy, the materials and actuation strategies discussed here have broader implications for the design of next-generation implantable medical devices, wearable health technologies, and adaptive soft machines that safely interface with living tissues. Continued progress in multifunctional materials, scalable fabrication, and intelligent control systems could accelerate the translation of soft robotic technologies across biomedical engineering and regenerative medicine.

1. Introduction

There are about 20.5 million individuals globally affected by heart failure, which remains one of the leading causes of mortality and a major global economic burden.[1] With global ageing populations and changes in lifestyle, the prevalence of heart failure is projected to increase by approximately 20%, with a significant proportion of cases progressing despite pharmacological and lifestyle interventions, making it necessary to find ways to help patients who have failing hearts live a reasonably normal life, especially in end-stage heart failure, where the patient experience severe limitations in functional capacity and daily activities.[2–4]

[a] School of mechanical and manufacturing engineering, University of New South Wales, Sydney, Australia. E-mail: J.Foroughi@unsw.edu.au
[b] School of Biomedical Engineering, University of Wollongong, Wollongong, NSW, Australia
[c] School of Aerospace, Mechanical and Mechatronic Engineering, Faculty of Engineering, University of Sydney, Australia
[d] School of Clinical Medicine, University of New South Wales, St Vincent's Private Hospital Sydney, Sydney, Australia
[e] Department of Cardiothoracic, Transplantation, and Vascular Surgery, Hannover Medical School, Germany

There is a scarcity of donors for heart transplantation, which remains the gold standard treatment for end-stage heart failure.[5] Ventricular Assist Devices (VADs) offer mechanical circulatory support and have improved survival, but their use is associated with complications such as thrombosis, bleeding, and the need for long-term anticoagulation.[6]

There is general agreement that developing viable and cost-effective alternatives to transplantation is essential. Recent advances in soft robotics raise the question of whether these technologies could provide viable pathways for developing efficient direct cardiac compression (DCC) devices for mechanical cardiac support (MCS). Exploring such systems requires a detailed understanding of the human heart across molecular, cellular, and organ levels, which provides valuable insights (Fig. 1).[2,7,8]

1.1. The human heart

The human heart is a fist-sized ≈350-gram organ largely composed of four principal cell types: myocytes, endothelial cells, fibroblasts, and smooth muscle cells. By cell number, cardiomyocytes constitute approximately 30–40% of the cells in the adult human heart, although they occupy the majority of the myocardial volume due to their large size.[9] These cardiomyocytes have very limited regenerative capacity, with an annual turnover of approximately 1%. Cardiomyocytes are composed of highly organised myofilaments containing the contractile proteins actin and myosin, which generate coordinated sarcomeric shortening and enable the heart to pump approximately 6 litres of blood per minute in a healthy adult at rest.[9] This contractile function depends on tightly regulated excitation–contraction coupling and intracellular calcium

Javad Foroughi

Prof. Javad Foroughi is a Visiting Professor at Hannover Medical School, Germany, and a Senior Research Fellow at the University of New South Wales, Australia. His research focuses on developing artificial muscle–driven soft robotic cardiac sleeves for non-blood-contact mechanical support of the failing heart. He specialises in smart materials, soft robotics, and wearable biomedical devices. He is internationally recognised for pioneering torsional carbon nanotube artificial muscles (Science, 2011). Prof. Foroughi has authored over 250 publications, secured more than $12 million in competitive funding, and supervised 25 PhD students, establishing leadership in translational soft robotic cardiac technologies.

Geoffrey Spinks

Geoffrey Spinks received his PhD in 1990 for his work on the mechanical behaviour of polymers and he has maintained a research interest in this area specialising in mechanical actuator materials (artificial muscles) and their applications. Geoff is currently Senior Professor in the School of Engineering at the University of Wollongong (UOW). Geoff has had a strong engagement with teaching across all levels of engineering materials and was co-founder of UOW's bachelor degrees in Nanotechnology and UOW Makerspace.

Christopher Hayward

Prof. Christopher Hayward is the Director of Cardiology, and Clinical Heart Lung Stream Director at St Vincent's Hospital, Sydney. He is Director of the MCS Research Laboratory at St Vincent's Centre for Applied Medical Research, Conjoint Professor of Medicine at the University of New South Wales, and Faculty member at Victor Chang Cardiac Research Institute Sydney Australia. Research interests include the haemodynamics of cardiac failure and advanced heart failure management with particular interest in mechanical support devices.

Chun H. Wang

Chun Hui Wang is a Scientia Professor and the Head of School of Mechanical and Manufacturing Engineering at the University of New South Wales (UNSW), Australia. He leads a research team focused on multifunctional composites for extreme environment applications. As the Director of the ARC Research Hub for Connected Sensors for Health, he leads a team of around 60 researchers in developing and deploying wearable sensors for human health monitoring and preventative healthcare.

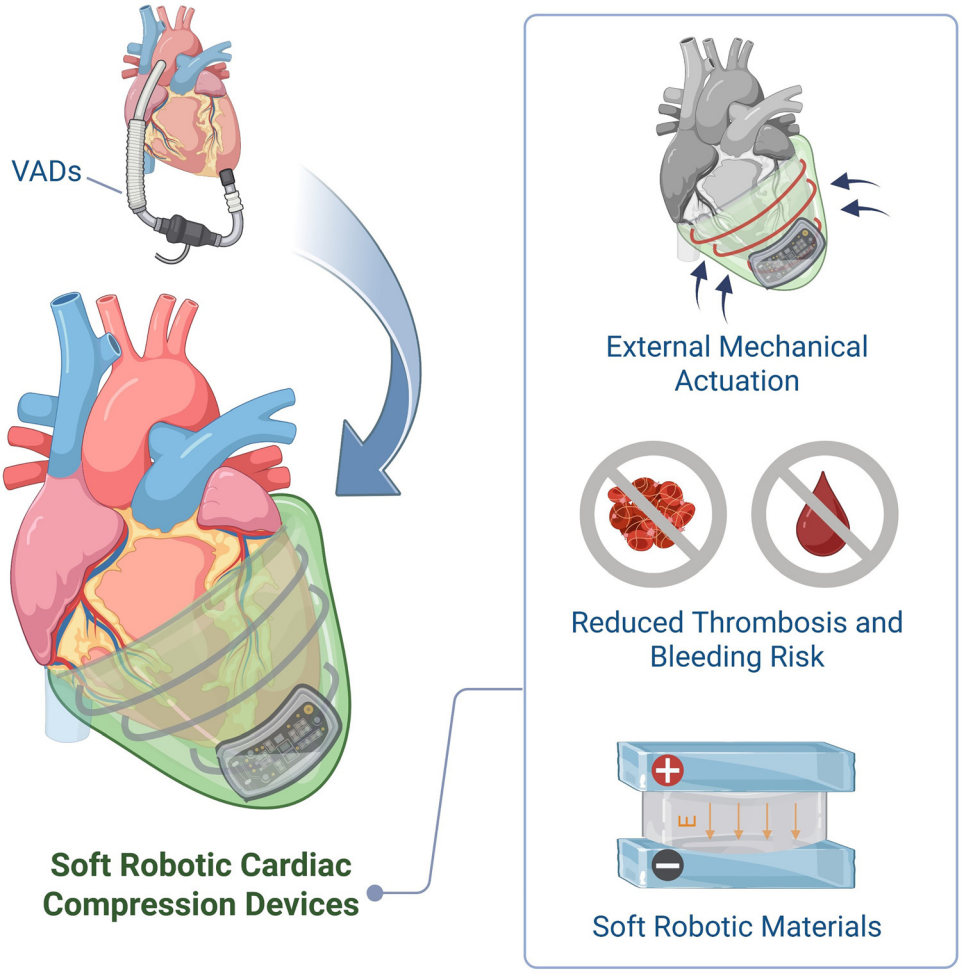

Fig. 1 Conceptual illustration of soft robotic direct cardiac compression (DCC) devices as an emerging alternative to ventricular assist devices (VADs) for mechanical cardiac support. Circumferential external actuation enables cardiac assistance without blood-contacting components, potentially reducing thrombosis risk while leveraging advanced soft materials for conformal interaction with the heart. Figure created with https://www.Biorender.com.

Arjang Ruhparwar

Prof. Arjang Ruhparwar graduated as a medical doctor from the University of Cologne, Germany, in 1994. After research at Indiana University, he completed cardiac surgery training at Hannover Medical School in 2004. He later joined the University of Heidelberg, where he led the Transplantation and Mechanical Circulatory Support program and served as Vice-Chairman of Cardiac Surgery. In 2019, he became Chairman at the University of Duisburg/Essen. Since April 2023, he has been Head of the Department of Cardiothoracic, Transplantation and Vascular Surgery at Hannover Medical School. His research focuses on aortic surgery, mechanical circulatory support, transplantation, tissue engineering, robotics, and regenerative therapies.

cycling, which ensure synchronous force generation across the myocardium. Regenerative capacity further declines with age, with turnover rates progressively decreasing in advanced age, a period during which the incidence of cardiac pathologies, including heart failure, increases significantly. While a reduction in the force-generating capacity of cardiomyocyte myofilaments is indicative of heart failure, this impairment arises from multifactorial alterations including disrupted calcium handling, sarcomeric protein modifications, cytoskeletal remodeling, and adverse ventricular loading conditions, and the precise molecular mechanisms remain incompletely understood.[7,10–12]

Importantly, the force generated at the sarcomeric level does not act in isolation but is transmitted through a highly organised myocardial architecture that determines global cardiac mechanics. The contractile behaviour of cardiomyocytes is organised within a highly structured myocardial architecture characterised by myocardial anisotropy, in which mechanical properties differ along longitudinal, circumferential, and radial directions.[13] This anisotropy arises from the helical arrangement of muscle fibres (fiber helicity), which rotate gradually from the endocardium to

the epicardium. The coordinated shortening of these helically oriented fibres generates ventricular torsion during systole, enhancing ejection efficiency and elastic recoil during diastole. These biomechanical features produce complex mechanical loading patterns across the ventricular wall, including circumferential compression, longitudinal shortening, and radial thickening.

These native helical fiber architectures provide an important biomechanical blueprint for sleeve design. Accordingly, several soft robotic sleeve architectures adopt helical actuator alignment and torsional compression pathways to better recapitulate physiological ventricular twist mechanics, which are central to efficient systolic ejection and diastolic recoil.[14,15]

Beyond cardiomyocytes, non-myocyte populations play a critical role in maintaining the structural and mechanical integrity required for this coordinated contraction. While the dominant cardiac myocytes are mainly responsible for contraction, fibroblasts function as a structural support network that contributes to extracellular matrix organisation and mechanical coupling.[16] However, under pathological stress, this balance shifts toward fibroblast activation and extracellular matrix remodelling. The proliferation of cardiac fibroblasts declines markedly after early development and remains low during adulthood under physiological conditions.[16] Their proliferation resumes in the heart during cardiac injury in response to growth factors and stress, leading to decreased contraction in that part of the heart. The decreased contraction results partly from the increased stiffness of the fibroblasts in comparison to the uninjured cardiac tissue. In addition, the stiffened fibroblasts further differentiate into myofibroblasts under mechanical and biochemical signalling cues through mechanotransduction, leading to scar tissue formation.[17,18]

These cellular and extracellular alterations directly translate into measurable changes in tissue-level mechanical properties. The stiffness of healthy cardiac tissues as indicated by the Young's modulus falls within 10–30 kPa. However, in ageing and infarcted tissues/cardiac injuries, the stiffness value is increased, with aged cardiomyocytes showing an increase to 35–50 kPa, while in infarcted tissues the stiffness increases go as high as 150 kPa.[11,17]

As myocardial stiffness increases and contractile efficiency declines, compensatory mechanisms are activated, which may initially preserve output but ultimately contribute to progressive failure.[19] The remaining functional cardiomyocytes also show decreased turnover in failing hearts. In these hearts, there is progressive decompensation that results in increased heart rate and decreased cardiac output, incomplete contraction of the overstretched muscles, and an overall increase in heart size.[20] When the ejection fraction is significantly compromised and inotropic agents are no longer sufficient, the heart is termed to be in advanced heart failure, and either transplantation or external support becomes crucial for the patient's survival.

The structural geometry of the ventricles further influences how these mechanical stresses are distributed.[21] The left ventricle, with the greater workload, has thicker walls (about 10–15 mm in healthy adults) and a conical shape, while the right ventricle has thinner walls (about 3–5 mm) and a crescent shape. The thickness of the left ventricle makes it less prone to distension when supported externally because of its greater stiffness (Fig. 2).[22]

Taken together, the progressive decline in sarcomeric force generation, adverse ventricular remodeling, and increased myocardial stiffness disrupt the mechanical equilibrium required for efficient cardiac output. While pharmacological therapies may temporarily modulate neurohormonal pathways and loading conditions, they do not directly restore contractile mechanics or reverse structural deterioration in advanced disease. Consequently, when compensatory mechanisms fail and ventricular geometry becomes maladaptive, mechanical circulatory support emerges as a necessary strategy to either augment or replace the failing pump function of the heart.

2. Currently available mechanical cardiac support devices

The mechanical support devices for supporting failing hearts have gradually evolved over the years. Currently, some have short term use as a bridge to heart transportation (BTT), and others serve as a destination therapy and only very few devices have attempted to replace the heart in its entirety aside from human heart transplantation. The latter is referred to as total artificial hearts (TAHs) while VADs refer to support devices that are mechanical pumps which are surgically implanted in the abdominal space with some form of attachments to the heart to provide ventricular support to the heart.

From an engineering perspective, mechanical circulatory support strategies can be broadly classified according to whether they completely replace native cardiac function or augment residual ventricular performance. These approaches differ fundamentally in their interaction with myocardial mechanics, blood-contact interfaces, and long-term physiological adaptability.

2.1. TAH

(TAHs) represent the most radical form of mechanical circulatory support, as they aim to fully replace the structural and functional role of both ventricles. The history of TAHs dates back to 1948, when Dr Sewell attempted to build a pneumatically powered TAH. The first successful clinical implantation was in 1969 with Dr Liotta's Liotta heart, a TAH (Fig. 3) that was used as a 64-hour bridge to transplantation where the patient died after 32 hours from sepsis and other complications.[23–25] With the advent of time, human transplantation improved, and the use of TAHs was restricted to BTT. A new surge in interest occurred in 1985, when the Jarvik 7 TAH (Fig. 1) was successfully used as BTT. More recently, the Syncardia® TAH (formerly Cardiowest® TAH) was built in 2002 and it recorded 79% one year post survival success and till date, about 1400 have been implanted.[24] Unlike assistive technologies that preserve native myocardial tissue, TAH systems eliminate intrinsic ventricular compliance, electromechanical coupling, and physiological

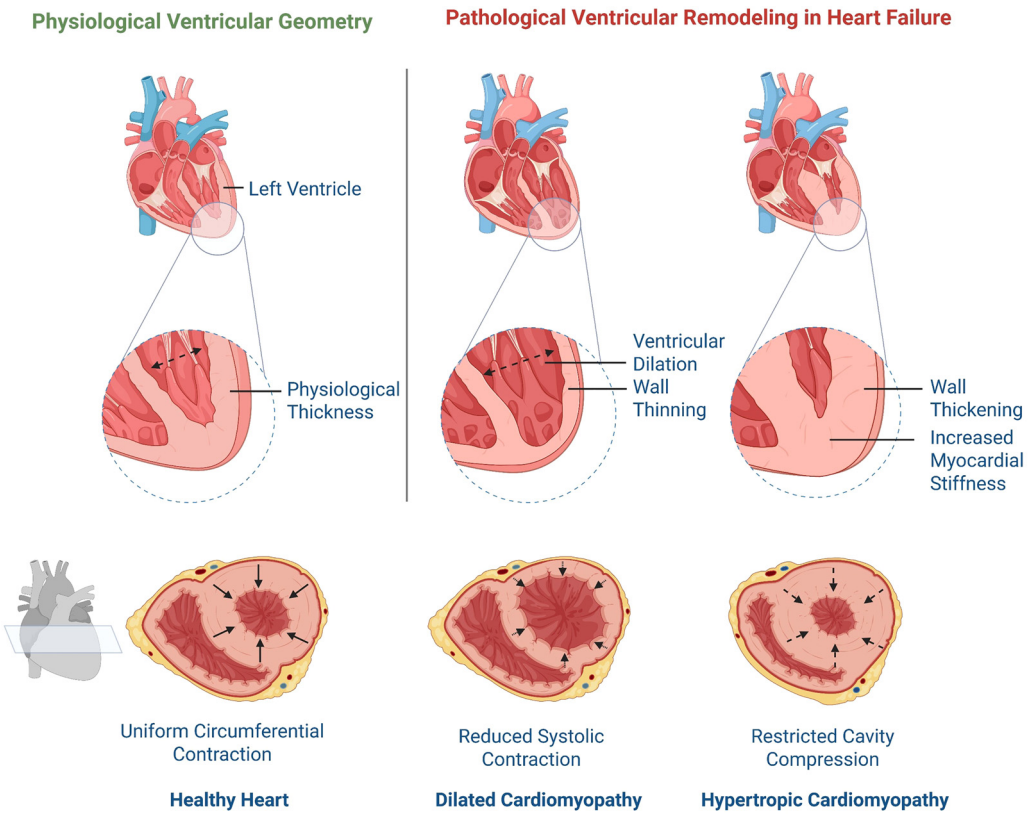

Fig. 2 Physiological ventricular geometry and pathological remodelling patterns in heart failure and their associated mechanical consequences. In the healthy heart (left), coordinated myocardial contraction preserves physiological wall thickness and chamber geometry, producing uniform circumferential contraction during systole. In dilated cardiomyopathy (centre), ventricular dilation and wall thinning reduce systolic contractile efficiency, resulting in diminished inward circumferential compression. In hypertrophic cardiomyopathy (right), ventricular wall thickening and increased myocardial stiffness restrict cavity compression and impair diastolic filling. The lower cross-sectional views illustrate the corresponding mechanical loading patterns, highlighting how structural remodelling alters circumferential force generation and ventricular biomechanics. Figure created with https://www.Biorender.com.

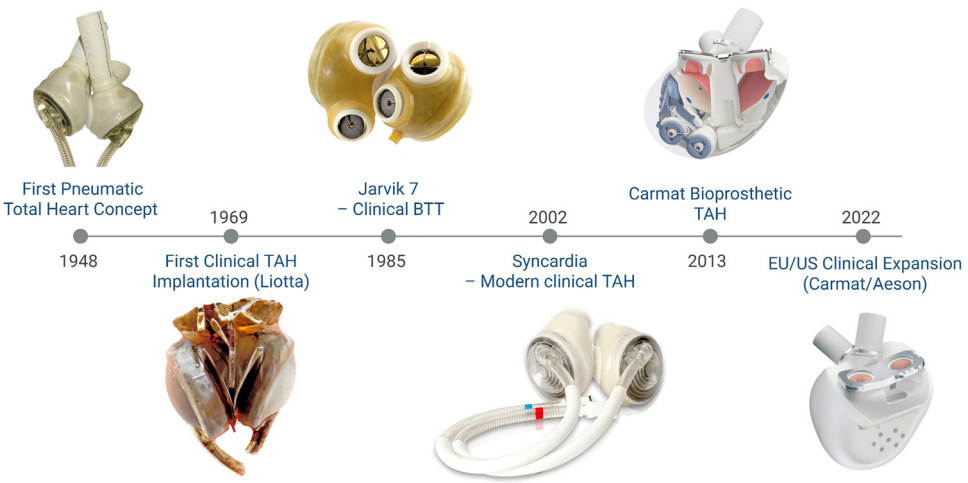

Fig. 3 Evolution of total artificial heart (TAH) systems from early pneumatic concepts to modern bioprosthetic designs. Timeline illustrating key milestones in the development of full cardiac replacement technologies: early pneumatically driven concepts (1948), first clinical TAH implantation using the Liotta heart (1969), Jarvik 7 clinical deployment as bridge to transplantation (1985), Syncardia TAH representing modern clinically adopted systems (2002), introduction of the Carmat/Aeson bioprosthetic TAH (2013), and subsequent EU/US clinical expansion (2022). These systems reflect progressive engineering refinement in materials, actuation mechanisms, and portability; however, they continue to rely on complete ventricular replacement and blood-contacting interfaces. Iotta heart reproduced under terms of the CC0 Licence, copyright 1976, National Museum of American History, Smithsonian Institution.[27] copyright 1976 from the collection of the National Museum of American History, Smithsonian Institution and B is The Jarvik 7 reproduced under terms of the CC-©0 License[28] copyright 1980 Papworth Hospital published by the Science Museum UK.

torsion, replacing them with mechanically driven pumping chambers.

There have been steady improvements, as seen in the Abiocor® TAH, which allows patients with TAH to leave the hospital with an internal battery lasting 30 minutes and an external battery lasting 4 hours. The Syncardia® was introduced in 2010, with the freedom portable driver to power TAH and enable patients to move around easily as the portable driver can be charged anywhere. Despite the progress, the TAHs are very prone to complications, (Abiocor® went out of production due to complications) and are expensive (costing up to 200 000 us dollars).[24,26]

While these technological refinements improved portability and short-term survival outcomes, the fundamental challenge of replicating the heart's preload responsiveness, mechano-adaptive regulation, and complex ventricular biomechanics remains unresolved. Despite technological refinements, TAH systems fundamentally eliminate native myocardial compliance, electromechanical coupling, and physiological torsion. Their reliance on blood-contacting surfaces introduces risks of thrombosis, infection, and haemolysis, while device size, cost, and driveline dependency limit widespread applicability. Moreover, the reliance on blood-contacting surfaces introduces persistent risks of thrombosis, infection, and haemolysis, while the surgical burden and device size limit broader applicability.

2.2. VADs

There has been greater clinical success with devices designed to support one or both ventricles than with total heart replacement systems. A ventricular assist device (VAD) typically comprises a mechanical pump, an inflow cannula, an outflow cannula, a percutaneous driveline, an external controller, and a power source. The pump partially or completely supplements the pumping function of the failing ventricle. The pump consists of a motor and an impeller or rotor; the motor drives the rotor to propel blood forward. For left ventricular support (LVAD), the inflow canula is inserted in the apex of the left ventricle to draw blood to the pump, while blood passes out to the ascending aorta through the outflow graft. In the right ventricle (RVAD), the inflow canula implantation is more complicated because of the risk of obstruction due to the unique anatomical features of the heart, the blood passes out to the outflow graft connected to the pulmonary artery.

The pump is implanted in the abdominal space below the diaphragm and has a driveline that connects to the power supply and the controller unit, which are outside the body. The device includes the pump, the inflow and outflow cannulas, the driveline connection, external battery pack and the controller unit, which all amount to about 3.5 kg in weight. The metallic parts are made of titanium and include the casing of the pump, the impeller, the connector cuffs of the input and output cannulas, driveline interface and internal bearings or magnetic parts.

VADs largely have three pump types: positive displacement, centrifugal, and axial flow. The first-generation positive displacement pumps were largely mechanical and designed to imitate the natural cardiac cycle using pneumatically driven pulsatile flow systems. Examples include the Thoratec Pneumatic VAD (Fig. 4). The devices were enormous in size, prone to fatigue, noisy, with a high morbidity rate.[29,30]

With further refinement, the second generation VADs were designed to address some drawbacks of the first-generation devices. The second-generation devices used axial

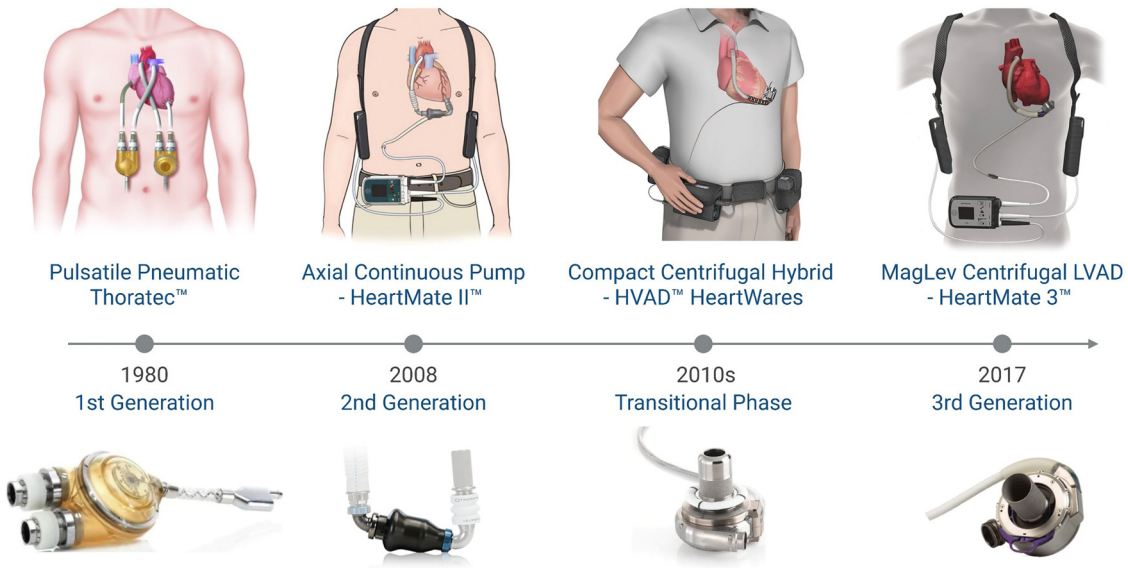

Fig. 4 Generational evolution of durable ventricular assist devices (VADs). Representative systems illustrating the progression from first-generation pneumatically driven pulsatile positive-displacement devices (Thoratec™, 1980s) to second-generation axial continuous-flow pumps (HeartMate II™, 2008), transitional compact centrifugal systems (HVAD™, 2010s), and third-generation fully magnetically levitated centrifugal devices (HeartMate 3™, 2017). The lower row highlights representative pump architectures corresponding to each phase of development. Device images are reproduced with permission of Abbott and Medtronic where applicable. © 2025 Abbott. All rights reserved.

and continuous-flow pumps that were smaller and more durable, providing a steady stream of blood *via* a rotating impeller. The devices were non-pulsatile; for example, the Heart Mate II had dimensions that were only 14% of those of the earlier device and weighed only a quarter as much. It used a continuous-flow pump, like most second-generation devices, and was approved for use as BTT in 2008 and DT in 2010, with an 85% survival rate one year post-implantation. More than 26 600 HeartMate 2 devices have been implanted.[30–32]

The rotor in second generation VADs had direct blood contact and had a textured lining titanium coating to decrease the risk of thrombosis (the clotting of blood that results from the metallic parts being seen as foreign by the body thereby triggering coagulation). The efficiency of the device was also improved and the reservoir chamber removed.[33] The devices, however, provided non-pulsatile flow, leading to weak or no pulse detection in patients; the axial flow also predisposed patients to shear stress.

Centrifugal flow VADs are classified as second generation in some publications, while others refer to them as third generation. The devices have a disc with blades spinning in a cavity. The replacement of bearings in the magnetic-suspension rotor was intended to reduce the risk of thrombosis by eliminating metallic bearings and reducing the wear-and-tear effects of the bearings. An example is HVAD by Medtronic, which is a continuous flow device. They have a centrifugal-flow device with a magnetically levitated rotor system; hence the reference to it as a third generation VAD.[31,34]

Third generation devices include the HeartMate 3™ (Fig. 4) and Heart ware HVAD. They are smaller in size than previous devices with reduced blood contact. The bearings are non-contact which allows for rotation without friction and they use a fully magnetically levitated rotor system.[35] The Heart ware by Medtronic uses a centrifugal pump, the pump is affixed to the base of the left ventricle and improved blood flow but was stopped in 2021 due to neurological effects and device malfunctions.

A patient with a LVAD set to operate at 2700 rpm will produce the following parameters: a heart rate ($\approx$76 beats per minute), cardiac output (5 litres per min), aortic pressure (91 mmHg), pulmonary arterial pressure (22 mmHg), right arterial pressure (7.4 mmHg), end systolic left ventricular volume (160 mL), left ventricular diastolic volume ($\approx$200 mL) and a left ventricular pump flow (5.3 L min^{-1}), based on several studies using VADs of different types in patients. Largely the device is set taking into cognisance the specific patient conditions that may produce alterations.[36–40]

By mechanically unloading the failing ventricle and augmenting forward flow, VADs reduce ventricular wall stress and improve systemic perfusion; however, they do not restore intrinsic myocardial contractility or physiological torsional mechanics.

2.2.1. Clinical effectiveness and limitations of current VADs. The advancements and progress of VADs have been substantial, with further miniaturisation, longer life batteries, reduced noise and coatings to prevent thrombosis. As a result of these technological refinements, there have been more than 25 000 continuous flow LVAD implantations in the United States of America as of 2022. In Australia, about 50% of patients coming in for a heart transplantation have an LVAD implanted already. Globally, a steady increase in the use of VADs as destination therapy over bridging therapy has been observed. Despite this, VADs have not proved to be superior to heart transplantation, 5 years post implantation due to many complexities and adverse effects.[41,42]

There remains a long way to go as limitations like patient selection, cost, adverse effects, device failure continue to hamper their use and reduce quality of life of patients. A summary of the limitations is depicted in Fig. 5.

Hemostatic complications like Pump thrombosis, hemorrhagic stroke and non-surgical related bleeding remain a major issue with VADs. Thrombosis occurs when the body reacts by initiating clotting mechanisms as blood encounters the metallic constituents which may result in stroke and other undesired events. To largely combat this, patients are placed on anticoagulant therapy. The anticoagulants have undesired effects and further predispose patients to bleeding and gastrointestinal tract bleeding has been largely reported in up to 25% patients with VADs/blood thinners. Earlier reports were about 61%[43] and recently about 25%.[44]

The multifactorial nature of bleeding further complicates clinical management. The number of factors influencing gastrointestinal tract bleeding from pump thrombosis makes the selection of candidates for VADs more cumbersome. Pre-implantation, gastrointestinal tract bleeding varies with VAD type, patient age, female gender, history of previous bleeding, use of other medications like selective serotonin reuptake inhibitor/serotonin and norepinephrine reuptake inhibitor and blood sugar level, while dosage of aspirin, renal function, reduced aortic valve opening influence post-implantation bleeding.[44–47]

VADs also predispose patients to driveline infections at the point of insertion resulting in about 47% of patients coming down with unplanned readmissions. Implantations are carried out *via* sternotomy which is largely invasive, and the patients can experience infections at the driveline, canula or pocket points. The percutaneous driveline outlet is responsible for device control, power communication and power supply.[31,35]

Some other complications like extremity ischemia are associated with percutaneous impella devices because of the blockage of the femoral artery by the large size catheter used for access have also been reported.[48] In addition, the risk of neurological events like stroke is increased in patients with LVADs especially in the first year after implantation.

There is also the risk of right ventricular failure when LVADs are implanted, due to left ventricular unloading that may shift the interventricular septum towards the left and eliminate the septal contribution to proper ventricular contraction, leading to enlargement and a spherical right ventricle. This altered ventricular geometry may impair right ventricular function and compromise overall hemodynamics stability. There have also been reported cases of VADs causing heart rotation.[41,49]

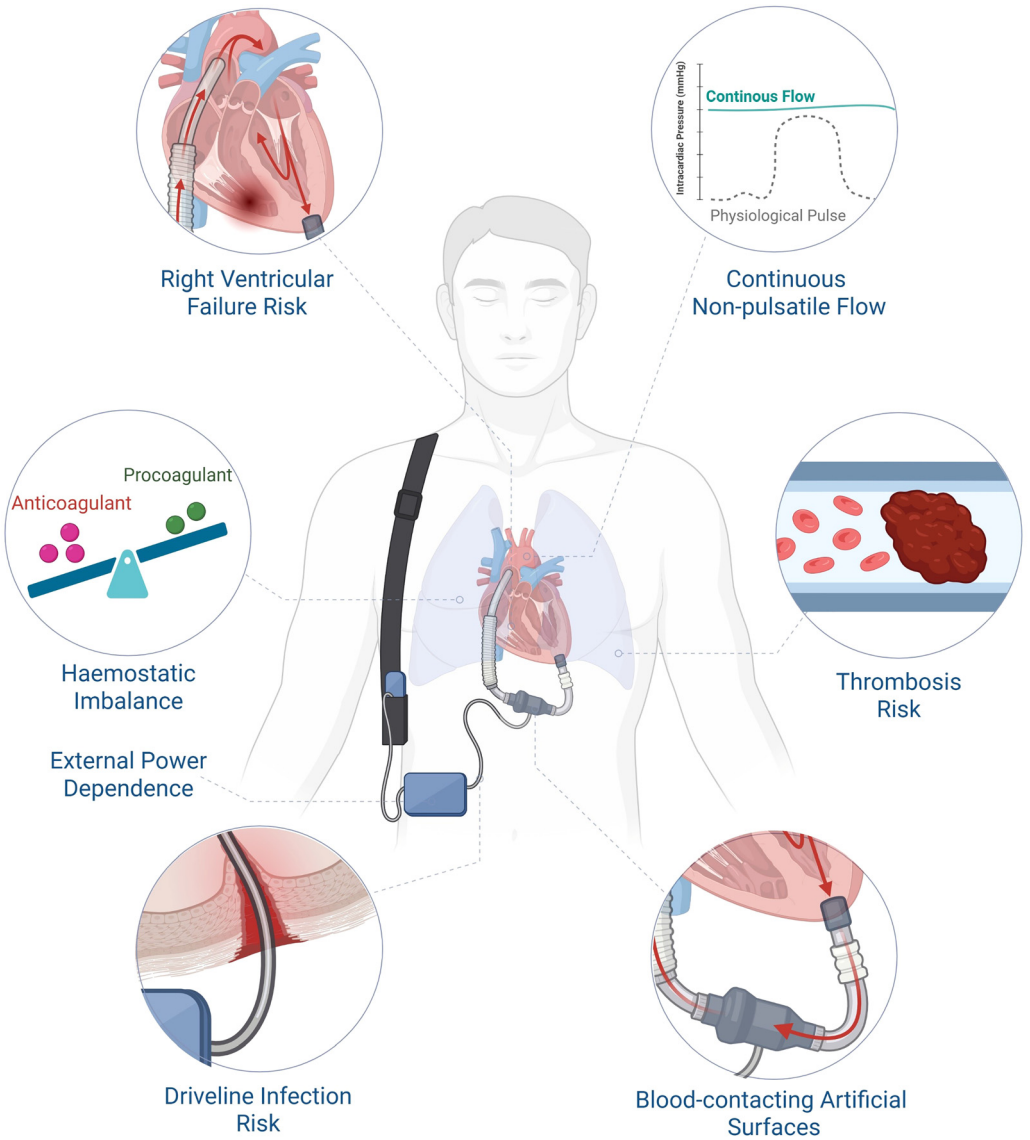

Fig. 5 Mechanistic limitations associated with durable ventricular assist devices (VADs). Schematic overview of key clinical complications arising from intravascular, blood-contacting, continuous-flow LVAD support. Persistent exposure of blood to artificial surfaces predisposes to thrombosis and necessitates long-term anticoagulation, contributing to haemostatic imbalance and bleeding risk. Continuous non-pulsatile flow alters physiological pressure profiles and may impair vascular and ventricular mechanics. Mechanical unloading of the left ventricle can increase right ventricular failure risk through septal shift and altered haemodynamic. Percutaneous drivelines introduce infection risk and external power dependence. Together, these features reflect intrinsic limitations of current rotary blood pump architectures. Figure created with https://www.Biorender.com.

Other limitations include cost, with the latest VADs costing up to 300 000 Australian dollars per patient as of 2023 where costs include device, hospitalisation, and readmission costs.[50] With size modification overtime, newer device pumps like the Heart Mate III weigh 200 grams as compared with previous devices like the Thoratec that weighed up to approximately 144 kg.[51,52] Given that the human heart weighs about 350 grams, an additional 200 grams is still bulky. In addition, when the weight of the control system and batteries are included, the devices are bulker getting up to 1.5 kilograms, making them largely uncomfortable for moving around. There is also the issue of space limitation in the abdominal region of pediatric patients and women for the pump implantation.

Currently, patients with VADs have difficulty measuring their blood pressure because of the absence of a palpable pulse. This is a direct consequence of continuous-flow physiology, further making patients rely on Doppler techniques for blood pressure measurement, making it difficult to empower patients to monitor and manage their own health or underlying conditions like hypertension.[53]

Taken together, while VAD technology has transformed the management of advanced heart failure, many of these complications are intrinsically linked to blood-contacting rotary pump design and continuous-flow haemodynamics. Considering the several challenges posed by VAD implantation and the pressure to find alternatives to transplantation, the investigation and

ongoing research into other viable pathways to provide mechanical support to the human heart are worth pursuing.

3. Desirable properties in VAD devices for managing heart failure

An ideal device for the management of heart failure must meet a wide range of criteria, which can be summarised as providing benefits comparable or superior to those of heart transplantation. Currently, no device provides superior benefits to heart transplantation, but some VADs are able to provide a 5-year survival rate post-implantation.[54] However, long-term superiority in terms of morbidity, quality of life, and complication burden has not been achieved. To provide similar or superior benefits to heart transplantation, the state-of-the-art assist device would improve cardiac parameters to the desired level as illustrated in Fig. 6. Importantly, these desirable properties arise directly from the mechanistic limitations discussed in the previous section. The limited use of metallic parts and minimal contact with the blood will significantly reduce the risks of thrombosis. Reducing or eliminating blood-contacting artificial surfaces would directly address homeostatic imbalance and thromboembolic risk. An ideal device will also encourage reverse remodeling, restoring physiological ventricular geometry and function rather than merely unloading the ventricle mechanically.

As summarised in Fig. 5, the ideal heart assist device should satisfy both physiological and engineering criteria. It should enable physiologically adaptive, pulsatile motion, thereby preserving native pressure–volume relationships and ventricular–vascular coupling. The device should incorporate limited or no metallic blood-contacting components and generate minimal thermal load, reducing inflammatory and thrombogenic responses. It should be lightweight, low-noise, and cost-effective, improving patient comfort and accessibility.

Durability is a critical requirement, with operational lifespan ideally extending to multiple years or exceeding billions of cardiac cycles, given that the human heart beats approximately 35 million times per year. The device should also operate with high energetic efficiency and low power consumption, reducing dependence on large external battery systems and improving patient mobility. Furthermore, implantation should involve minimal tissue disruption and reduced surgical invasiveness, thereby lowering perioperative risk and infection rates.

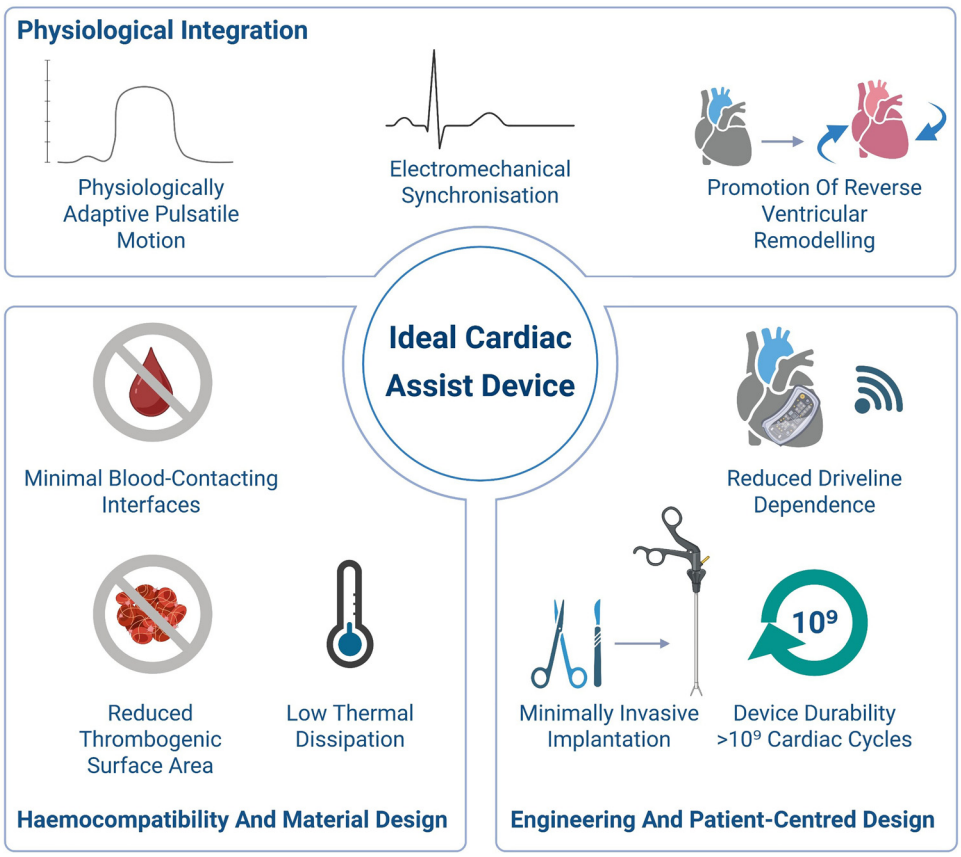

Fig. 6 Summary of desirable properties for ideal cardiac assist devices. An ideal cardiac assist system should integrate physiological compatibility, hemocompatibility, and engineering reliability. Key characteristics include physiologically adaptive pulsatile motion, electromechanical synchronisation with native cardiac rhythms, and the potential to promote reverse ventricular remodelling. From a hemocompatibility perspective, minimal blood-contacting interfaces and reduced thrombogenic surface areas are desirable, alongside low thermal dissipation. Engineering and patient-centred considerations include minimally invasive implantation, reduced dependence on external driveline systems, and long-term device durability capable of sustaining more than 10^9 cardiac cycles. Figure created with https://www.Biorender.com.

Collectively, these characteristics define a next-generation cardiac assist paradigm that moves beyond simple mechanical pumping toward physiologically integrated support. By addressing the intrinsic complications associated with continuous-flow, blood-contacting rotary systems, such an approach would aim not only to sustain life but to restore functional cardiac mechanics and long-term patient wellbeing.

4. Developments in soft robotic technology

Soft robots have continuously evolved to make their interaction with the human body friendlier and less rigid than that of traditional robots. Soft robots have been used to provide artificial limbs, surgical tools, biomimetic organs and in medical rehabilitation in stroke patients, spinal cord injury, multiple sclerosis, neurological disease and other conditions.[55,56]

With the human myocardial cells contracting about ≈10–20% during systole, rigid components like metals cannot adhere or conform to the heart's morphology, further making soft, pliant materials suitable for engineering DCC sleeves, hereafter referred to as soft robotic sleeves.[57] There have been many interesting approaches to engineering, such as soft, pliable patches and devices that provide direct epicardial compression on the human heart and aid failing hearts.

The potential advantages of DCCS over VADs are diverse. The first major advantage is the limited blood contact which significantly reduces the risk of thrombosis and the consequent need for anti-coagulants. Secondly, DCCS will eliminate the need for vascular access thereby reducing extremity ischemia and bleeding. Other potential advantages include maintaining arterial pressure pulse, cheaper devices, reduced risk of tissue damage, smaller sizes, noiseless operation, minimally invasive procedures, and ease of device deactivation as required.[58] Importantly, these features address several intrinsic limitations of continuous-flow, blood-contacting rotary pumps discussed in Section 2.

4.1. Overview of design strategies and soft materials

The human heart can typically be described as a biological actuator with integrated sensing and control systems. The heart muscles generate a strain up to 20% during systole, and an output stress of 50–100 kPa, generating about 1 Joule per heartbeat with a bandwidth frequency range of $<$10Hz, pumping about 5 litres of blood per minute at a pressure up to 150 mmHg.[59]

In response to the soft nature of biological tissues, soft building materials of synthetic, thermoelastic, or biological origin have found wide applications in DCCS and devices due to their ease of use, tissue friendliness, and tunability. Such soft materials can serve as building templates for actuator construction or for making sensors that can provide cardiac support. Examples include silicones and polyurethanes.

Silicones have a silicone–oxygen backbone and are flexible, biocompatible, and operate over wide temperature ranges. The elastomeric silicones offer the added advantage of biocompatibility and ease of modification as seen in current use as heart prostheses and hemodynamic catheters. Since silicones are naturally hydrophobic, improvements in the surface properties of the polymer have been achieved through the incorporation of additives such as polyethylene glycol, the grafting of other hydrophilic polymers onto the backbone, and surface coatings. The improvements serve to decrease protein reactions that can lead to thrombogenic reactions, and some of the modifications take into consideration the shear stresses of blood flow. An example of a practical application because of the biomimetic property of silicones is the use of silicone plugs in Heart Mate III VAD to prevent re-sternotomy after the initial procedure.[60]

Another applicable material is polyurethane, with strong potential for use in soft robotic sleeves or DCCS. Polyurethane has also been used in its expanded form, ePTFE, which is a fluoride resin made of carbon and fluoride, that is chemically inert with a low friction coefficient. The microstructure in the expanded form may, however, provide an environment for bacterial growth and interfere with haemostasis. In all its forms, PTFE has been used for vascular grafts, stent coatings and to make cardiac patches.[61]

Dacron, another soft material, is a type of polyester, polyethylene terephthalate, with a high elastic modulus and strength, and is resistant to degradation. It has been used to produce a variety of medical devices that support the voluntary muscles of the body. The liota heart was made from Dacron. A major drawback of using Dacron is the risk of late aneurysm[25,27]

Polyurethane, its expanded form, ePTFE, and polyesters are easily available, have low degradability and are biostable *in vivo*. Other examples of suitable polymers include polyethylene glycol, polycaprolactone, polyglycolic acid, PDMS-PU (polydimethylsiloxane polyurethane), and collagen.[61]

When constructing cardiac sleeves from these polymers, their material properties can be tailored to suit the desired application. A good example is silicone, with a wide range of high Young's modulus in comparison to muscle. The heart tissue has a Young's modulus ranging from $<$50 kPa to 100 kPa, depending on the heart's health, while the Young's modulus for medical grade silicone can range from about 10 kPa to 4000 kPa. The disparity in Young's modulus may result in local tissue stress when integrated into the human heart or cause a local non-conforming fit, but with modifications like adjustment of the reactive group ratios, a softer material with equivalent properties to heart tissue can be obtained. Also, the polymeric structure of silicone, apart from its Young's modulus, contributes to its softness, which has resulted in its wide application in cardiovascular devices. Another example is polyurethane, which can have its Young's modulus varied depending on the type and density, giving it a range from 1.5–5.5 10^4 kPa. Nylon 6, a polymeric material from which twisted and coiled polymers have been made, has a Young's modulus of about 2.5×10^6 kPa, which is much higher than the heart modulus but with modifications can be made

more tissue-friendly.[57] Some ionic polymer composites have lower Young's moduli, such as polypyrrole, which has a Young's modulus of 20–200 kPa in the hydrogel form but values can go up to 10^5 kPa depending on the oxidation state and doping level making some ionic polymer composites stiff for cardiovascular integration.[57,62]

Another interesting group of materials, hydrogels mimic the extracellular matrix, indicating their ability to simulate the complex physical, chemical, and biological environment surrounding cells in the body conferring tissue-friendly properties and making them potential templates for designing soft robotic sleeves.

In summary, polymeric materials for designing soft robotic sleeves should have features like durability, tissue friendliness, antithrombotic properties, resistance to infection and late degeneration. Some resistance to biofouling and surface coatings that allow sterilisation are also desirable.

Beyond intrinsic softness and biocompatibility, the successful translation of soft robotic cardiac sleeves depends on how material architecture helps address key device-level challenges. Conformal heart–device coupling is increasingly improved through modulus-tunable elastomers, anisotropic composite layouts, and patient-specific geometries that reduce local stress concentration while preserving native torsional motion.[63–65] In parallel, cyclic durability is addressed using fiber-reinforced actuator structures, multilayer elastomer composites, and fatigue-resistant thin films that minimise crack formation, delamination, and creep under repeated cardiac loading.[49,66] Materials also play an important role in physiological synchronisation, particularly through stretchable conductive pathways and compliant sensing layers that maintain signal fidelity during deformation.[67,68] Finally, power delivery remains closely linked to material choice, where actuator chemistry directly influences efficiency, voltage requirements, and the long-term feasibility of implantable systems.[67]

Representative examples discussed later in this review further illustrate this design logic. For instance, the modulus-matched silicone McKibben sleeve by Roche *et al.* improves epicardial conformity and torsional force transfer, while thin-film TPU systems such as CorInnova and reBEAT improve deployability and fatigue resistance.[49,66] Likewise, electroactive polymer platforms such as E-CAD demonstrate how actuator material chemistry can reduce power consumption and overall device bulk.[67]

Building on these examples, the performance of soft robotic cardiac sleeves is fundamentally governed by the structure–property relationships of the actuator materials themselves. In pneumatic elastomer systems, braid angle, fiber reinforcement geometry, and elastomer modulus directly determine radial expansion, axial shortening efficiency, and force transmission during circumferential compression.[69–72] In electroactive and dielectric elastomer platforms, film thickness, dielectric constant, compliant electrode composition, and multilayer stacking strongly influence Maxwell stress generation, actuation strain, voltage demand, and long-term dielectric stability.[63,67,73] For twisted-and-coiled polymer muscles, precursor fiber diameter, twist density, coiling pitch, and conductive coating design govern thermomechanical conversion efficiency, contraction speed, and heat dissipation.[74–77] Likewise, in shape-memory systems, alloy composition, phase-transition temperature, and filament dimensions affect force output, hysteresis, response speed, and cooling behaviour.[78–81]

4.2. Actuation mechanisms in soft robotic sleeves

Most DCCS or devices to date have largely used hydraulic, pneumatic or electrothermal actuators. The design of DCC sleeves involves several steps: selecting the actuator mechanism, selecting materials, fabricating actuators, designing the sleeve, testing the prototype, incorporating sensors, optimising pressure and force measurements, and exploring integration strategies. The history of external mechanical compression dates to the mid-1800s, when DCC was performed with the primary intent of providing resuscitation *via* cardiopulmonary access. Table 1 provides a summary of currently available devices and the actuation mechanisms.

4.2.1. Pneumatic/hydraulic robotic sleeves. Pneumatic actuation systems using the McKibben principle have been applied as DCCS. The actuation system uses compressed air (pneumatic) or fluids (hydraulic) to generate mechanical action while vacuum-driven actuators use negative pressure from vacuums to create mechanical motion or actuation. The operating principle in the pneumatic, hydraulic, and vacuum-driven systems involves air/liquid and positive/negative pressure-driven actuation.

In the pneumatic cardiac support devices, hydrogels, elastomeric materials, or plastics that interact well with the human body make up the pliant chambers which deform depending on their composition or design and eliminating rigid systems reducing the risk of tissue damage.[69]

The first documented DCCS device, the Anstadt cup, a pneumatic device, was made from silicone membrane and Pyrex shell and was used in 1965 by Anstadt and Kolobow for cardiopulmonary resuscitation originally. It was used as a pericardial cup to massage the heart and aid blood pumping. The anstadt cup was elliptically shaped to fit both ventricles. It used pneumatic pressure to deliver pulsatile pressure through the inflatable inner diaphragm. The pulsatile contractions were not synchronised with the native cardiac rhythm at the time due to limited technology. However, in 1996, it was used as a bridge to transplantation for 56 hours, and the success led to the development of the heart booster® by Abiomed. The use of DCCS in the management of heart failure commenced around 2010.[58]

Pneumatic DCCS have evolved from the Anstadt cup[70,71] to the Abiomed's Heart Booster,[72] to the robotic cardiac sleeve by Roche *et al.*,[63] then the CorInnova's minimally invasive cardiac sleeve by John Criscione and team,[64,65] and more recently, the ReBeat device.

The Abiomed® booster used was designed around 1999. It consisted of serially arranged compression tubes from inflatable polyurethane tubes coated with silicone, arranged around the heart in the shape of a cylinder to cover the ventricles.

Table 1 Overview of currently reported direct cardiac compression (DCC) soft robotic devices, summarising actuation mechanisms, material composition, motion types, operating conditions, control strategies, biocompatibility, clinical validation status, fixation approaches, and key device limitations. Abbreviations: LV, left ventricle; RV, right ventricle; BiV, biventricular; ECG, electrocardiogram; EF, ejection fraction; TPU, thermoplastic polyurethane; PEEK, polyether ether ketone

Actuation mechanism (material composition)	Motion type	Operating conditions/peak pressure/force output	Control strategy	Biocompatibility	Clinical status	Target chamber	Device features/ fixation	Area of improvement	Device citation
Pneumatic McKibben actuators (silicone and TPU sleeves)	Circumferential compression and helical twisting	Restores ~88% cardiac output; ~0.5 N actuation force at pressures up to 150 kPa	Closed loop feedback with pressure synchronised system	No inflammation in epicardial surface	Acute sheep model using esmolol-induced cardiac failure demonstrating restoration of cardiac output	LV	Epicardial suturing	Large device size; requires invasive sternotomy for implantation	3D Robotic cardiac Sleeve[63]
Pneumatic McKibben actuator (TPU chambers with aluminium frame and PEEK ventricular frame)	Twisting and circumferential compression	65.5 g (RV device) and 38.7 g (LV device); actuator force 14–18 N at ~10 psi inflation pressure	Closed loop, pressure sensing catheter	No significant damage reported	Acute pig model (n = 4); restored blood flow and pressure from baseline heart failure conditions; LV aortic flow increased from 39% to 116% of healthy baseline	LV/RV	Customised ventricular frame; septal bracing; sutured to inter-ventricular septum	Device size: implantation requires invasive sternotomy	Robotic Cardiac Sleeve[73]
Pneumatic dual-chamber (thin-film TPU actuator with nitinol frame, comprising inner saline-filled and outer air-filled compartments)	Direct epicardial compression	Operating pressure ~20 kPa	Closed loop, ECG sensing	Superficial inflammation[66]	Sheep (n = 3) with EF increase from 20% to 31% and ~1 L min^{-1} increase in cardiac output; paediatric proof-of-concept in goat; 14 days in chronic failure; undergoing regulatory evaluation	BiV	Minimally invasive fixation; saline layer adhesion to epicardium (no sutures required)	Limited size customisation	CorInnova[58,64–66]
Pneumatic inflatable bladder system with two chambers	Synchronised epicardial pulsation	Up to 15 mmHg increase in LV pressure; ~20 ml reduction in LV volume during actuation	ECG synchronised pulsatile control	No inflammation, no arrythmias, no ischemia	Acute pig tests (n = 5) and chronic pig tests (n = 2); tested in live animals for 30 days; first feasibility human trial in 2025 successful as bridge-to-transplant	BiV	Subxiphoid surgical access	No major limitation reported	reBEAT by AdjuCor GmbH[49]
Pneumatic silicone epicardial patch actuators with dual chambers	Epicardial adhesion and pericardial inflation/ deflation		Closed loop ECG sensing *via* sonomicrometry heart dimension sensing	—	Sheep model (n = 12): 6 control and 6 infarcted animals, Sheep model (n = 10) using esmolol-induced heart failure; open-chest model.[82]	BiV	Epicardial fixation using 3-0 and 5-0 prolene sutures; negative-pressure adhesion	—	Heart Patch[58,82]
Pneumatic balloon catheter actuator enabling	Cyclic pulsatile compression	—	Synchronisation with native ECG	—	Human trial: 2 patients; EF improved from 30–45% in patient 1 and 5–30% in patient 2; implantation duration 5 days		Intrapericardial fixation	—	Percassist by Percassist Inc balloon cathether[83]
Electroactive polymer actuators (pre-stretched acrylic elastomer with carbon/ silicone electrodes and bias springs embedded in TPU/silicone)	Circumferential compression	<60 g device weight; 0.3 W power consumption; 5.5 kV actuation voltage; force 5–6.7 N	Open loop control	No inflammation	*Ex vivo* porcine test model; EF increase from 39% to 43%	BiV	Patient-specific ventricular customisation	High voltage requirement; hysteresis	E-CAD[67]

Table 1 (*continued*)

Actuation mechanism (material composition)	Motion type	Operating conditions/peak pressure/force output	Control strategy	Biocompatibility	Clinical status	Target chamber	Device features/ fixation	Area of improvement	Device citation
Hydraulic actuation using silicone tubes	Circumferential and twisting compression	~ 25.3 N compression force (*in vitro* silicone model); ~ 39.5 mmHg pressure in *ex vivo* porcine heart	Sinusoidal signal input	Artificial pericardium used to prevent bruising of the pericardial surface	*Ex vivo* porcine heart model	BiV	Friction-based fixation; small tubing system with 0.3 mm driveline	Improved fixation strategies required; prevention of air pockets	Robotic cardiac sleeve[22]
Electrothermal twisted-and-coiled polymer artificial muscles (silver-coated nylon-6) with silicone insulation	Circular contractile motion	Heating to ~ 80 °C; ~ 32.5 V input; pressure up to ~ 120 mmHg using parallel actuators (~ 2.4 N force)	Open loop with potential for closed loop		*Ex vivo* lamb heart model	BiV	Lightweight and portable design	High actuation temperature	Cardiac sleeve[56]

The tubes inflated to provide systolic compression and deflated during systole when positive pneumatic pressure was applied. The tubes were filled with fluid during the half cycle and improved cardiac output. The device could use either a hydraulic or pneumatic pump system and was used to pump up to 6.5 litres per minute in calves.[22,72]

In 2017, the 3D soft robotic cardiac sleeve[63] used McKibben actuators embedded in silicone, with tubular muscle filaments arranged in helical and spiral shape to mimic the muscular arrangement of cardiac tissues. It also simulated the natural cardiac muscles helical twist and circumferential pattern. The device reestablished 88% cardiac output in pig models and the sleeve was designed to have the same stiffness value as the human heart.[63]

A slightly different approach was engaged by[73] who fabricated a sleeve that was anchored to the ventricular wall and interventricular septum in an effort to eliminate mechanical desynchronisation between the septum and the free wall of the ventricles, which may not be corrected by direct external cardiac contraction. McKibben pneumatic artificial muscle concept was used for making the device and a thermoplastic elastomer TPE bladder was shaped using a heat press and contained a mesh structure that contracted linearly and expanded radially when the bladder was pressurised.[73]

Also in 2017, the Corinnova device was invented; it was more portable than previous pneumatic devices, with minimal invasion required for implantation. The CorInnova's minimally invasive cardiac sleeve self-deploys around the ventricles. It features thin-film pneumatic chambers containing nitinol wire, which act as a shape-restoring scaffold, allowing the device to collapse for minimal invasiveness. In *in vivo* studies, the device improved cardiac output by 50%. The collapsible sleeve self-wraps around the heart, beats in synchrony with it, and is powered by a pneumatic drive.[64,65]

More recently, the reBEAT device by AdjuCor GmbH (Fig. 7), is a pneumatic device, that the proof of concept showed how it can be customised by utilising the end diastolic CT scan of the patient's heart to obtain a 3D print model. The device comprises a thin cardiac sleeve $\approx$1.2 mm thick, containing three pneumatic chambers with electrodes for ECG detection: 2 encircling the left ventricle and 1 the right ventricle, providing biventricular support. The cushions are made from polyurethane. The device has been designed to provide support for up to 2 years with about 80 million cycles in benchtop models. The device is foldable to minimise the invasiveness of implantation. The inflation and deflation synchronise with the ECG R and T waves. The device co-pulsates and has a driveline connected to a drive unit.

Overall, pneumatic systems are versatile, easy to operate and achieve a high actuation force similar to that of natural muscles. Despite the ease of operation, some drawbacks of pneumatic systems include the massiveness of size to achieve desired actuation speed, and low efficiency. Pneumatic heart assist devices like the one by Roche *et al.* are dependent on pneumatic power sources, which have large compressors and drivelines, and are noisy in operation. There is also a risk of air

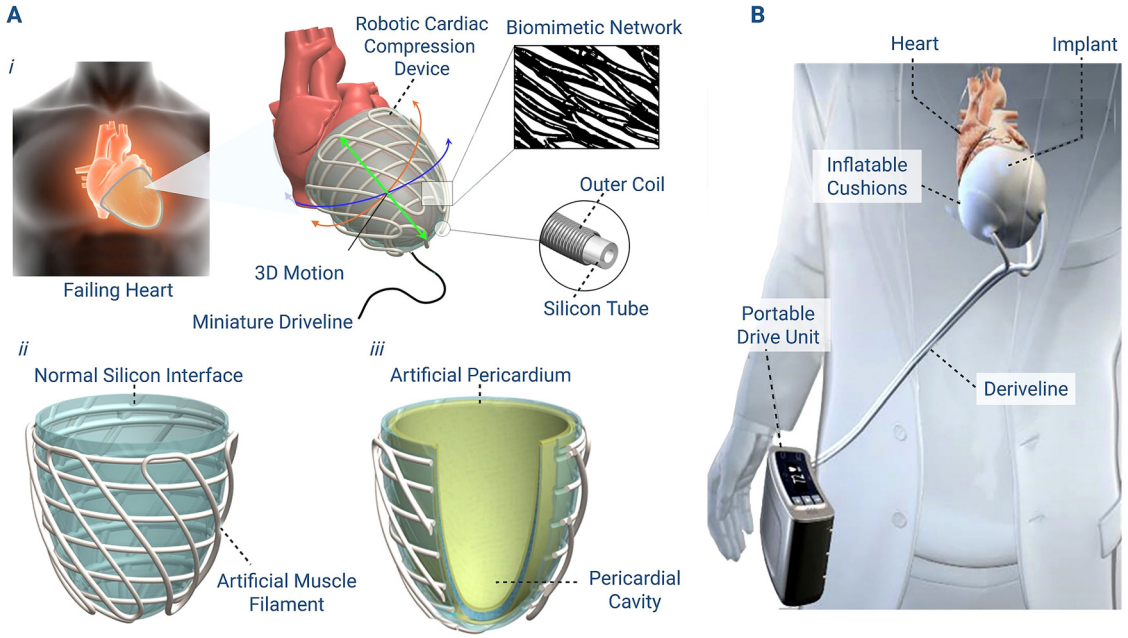

Fig. 7 Representative soft robotic direct cardiac compression systems. (A) Hydraulic actuator-based direct cardiac compression sleeve (DCCS) design adapted from Phan *et al.*,[22] illustrating (i) the robotic cardiac compression device positioned around a failing heart, (ii) artificial muscle filaments embedded within a compliant silicone interface, and (iii) integration within an artificial pericardial cavity to enable biomimetic three-dimensional motion. The system utilises fluid-driven artificial muscle filaments to generate radial, circumferential and torsional compression without direct blood contact. Reproduced under the terms of the CC 4.0 licence from Phan *et al.*, Advanced Intelligent Systems (2025). (B) ReBeat intrapericardial pneumatic device currently undergoing clinical evaluation,[49] demonstrating inflatable cushions, portable drive unit and percutaneous driveline. The device provides synchronised biventricular support *via* ECG-triggered pneumatic actuation without intracardiac blood-contacting components. Reproduced with permission from The Journal of Thoracic and Cardiovascular Surgery, 166(4), 2023. Figure created with https://www.Biorender.com.

embolism during implantation.[63] They may also not be as precise as electric motors, and can be prone to hysteresis, and scalability issues may also arise; scalability issues refer to compromised speed and responsiveness when size of tube is increased, and larger soft actuators can exhibit complex non-linear deformation behaviours. The devices may also generate heat while operating just like VADs.[67,69,74]

The Abiomed's Heart Booster utilised fluids for actuation. Although more force is required for hydraulic actuation, it is generally favoured for DCCS as leakages can be easier to contain in case of device malfunction.

A recent research by[22] also used fluid driven actuation (Fig. 7B). The soft robotic device has a soft inner silicone shell, semi-spheroidal in shape, and an outer shell made from hydraulic artificial muscle filaments (silicone tubes inside a restrictive coil spring with one blocked end). To replicate native heart contractility, multiple filaments are braided to produce radial, axial, and torsional compression. The device generated a pressure of about 50 mm Hg and achieved a stroke volume of 70 ml per heartbeat.[22]

4.2.2. Electrothermal soft robotic sleeves. An attempt has been made to use electrically and thermally actuated soft sleeves to provide direct mechanical support to the heart. An artificial muscle sleeve wrapped circumferentially around a heart model has been used to generate desirable cardiac parameters. The sleeve was made from twisted and coiled polymer muscles.[56]

These types of actuators gained significant research attention around 2011 and are made from commonly available polymeric materials such as nylon 6. They have been extensively investigated at the individual muscle level, making it easier to compare them to individual cardiac muscles. In studies, they surpassed individual cardiac muscles in force generated, displacement, and actuation speed, and outperformed human skeletal muscles in power output, with an output about 20 times that of human muscles under controlled experimental conditions. They can generate a contractile force up to 100 times human muscles of similar length and weight and have generated up to 5.3 kW kg^{-1} with little to no hysteresis.[75–77]

The twisted and coiled polymer muscles can serve as building blocks in DCCS or devices to replicate the complex native contractility of the human heart with proper study and customisation. The lightweight and low voltage requirements make them more suitable compared to pneumatic actuators and dielectric elastomers.[84]

In a previous attempt to provide DCC using twisted and coiled polymers (Fig. 8), each electrothermally actuated twisted and coiled polymer actuator generated about 7.1% contraction and a maximum stress of 433 KPa. The performance metrics compare well to those of a cardiac muscle that is documented in a recent study. The maximum reported stress in isometric condition for cardiac muscle was 9.2 KPa with a maximum contraction of 6.9 ± 0.9% in isotonic condition for a muscle strip. The major drawbacks of twisted and coiled polymer

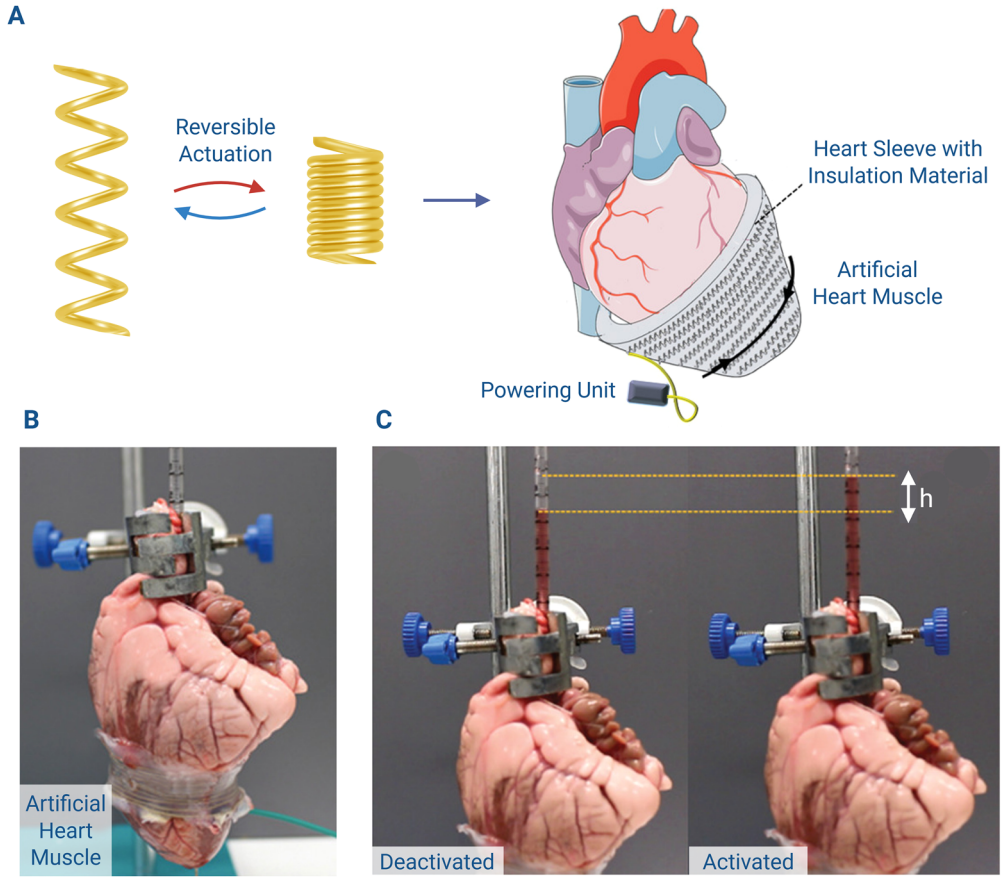

Fig. 8 Twisted and coiled polymer artificial muscles for cardiac assist applications. (A) Actuation principles of twisted and coiled polymer muscles under different electrical and thermal triggers. (B) Conceptual illustration of a cardiac assist sleeve configuration. (C) Electrothermal actuators wrapped around an *ex vivo* cardiac model. Images B and C are reproduced under the terms of the CC 4.0 licence (© 2025) from High Performance Artificial Muscles to Engineer a Ventricular Cardiac Assist Device and Future Perspectives of a Cardiac Sleeve,[56] published in Advanced Materials Technologies. Figure created with https://www.Biorender.com.

artificial muscles are the high operating temperature, slow cooling rate and low efficiency of the system.[56,85]

4.2.3. Electroactive polymer actuators. Electroactive polymer actuators are another interesting group of artificial muscles that are soft, lightweight, and can undergo large deformations, and are largely classified into two groups: ionic and electronic actuators. Electroactive polymers (EAPs) are broadly divided into electronic systems, such as dielectric elastomers, and ionic systems, including conductive polymers and ionic polymer–metal composites (IPMCs), which differ fundamentally in their actuation mechanisms and operating voltages.

Dielectric elastomers (DEA) are thin elastomer films sandwiched between two compliant electrodes and operate by a decrease in the elastomer film thickness when voltage is applied to the membrane, resulting in high strain levels and expansion in-plane. Some properties like their fast actuation speed and lightweight, large strains, pulsatile deformations, high efficiency, biocompatibility, and the ability to be customised to meet a desired need, make them suitable templates for a soft robotic sleeve for mechanical cardiac compression (Fig. 9A).[78]

In a recent research work using DEA actuators as a DCCS (Fig. 9B), a portable sleeve, called E-CAD, from DEA, weighed less than 60 g, with an outer diameter of just 0.3 mm at the insertion site.[67] The device used units of a pre-stretched acrylic electroactive polymer, 3M, VHB 4910, with a painted silicone, carbon black powder, and hexane as the electrodes in a ratio of 15 : 1 : 150. It was coupled to a negative bias spring (NBS), and enveloped in a thermoplastic polyurethane (TPU) flexible sleeve, that was further embedded in silicone. The NBS was made from thin steel springs. The cardiac sleeve was tailored to suit the varying stiffness of the heart region, as is common in failing hearts. The E-CAD worked in synchrony with the heart, activating during systole and deactivating during diastole to allow cardiac filling. Planar expansion is observed when voltage is applied, as the EAP softens, which causes the heart to contract, when the device is deactivated, EAP hardens and the spring is compressed and the heart is allowed to expand. This actuation mechanism is governed by Maxwell stress, whereby the applied electric field induces electrostatic compression through the film thickness and lateral expansion in-plane.

When the e-cad was applied to a silicone heart failure phantom, an improved ejection fraction from 39 to 43% was observed at 5.5 kV. The device consumed about 0.3 W and operated at up to 5.5 kV, as is characteristic of EAP, but at a

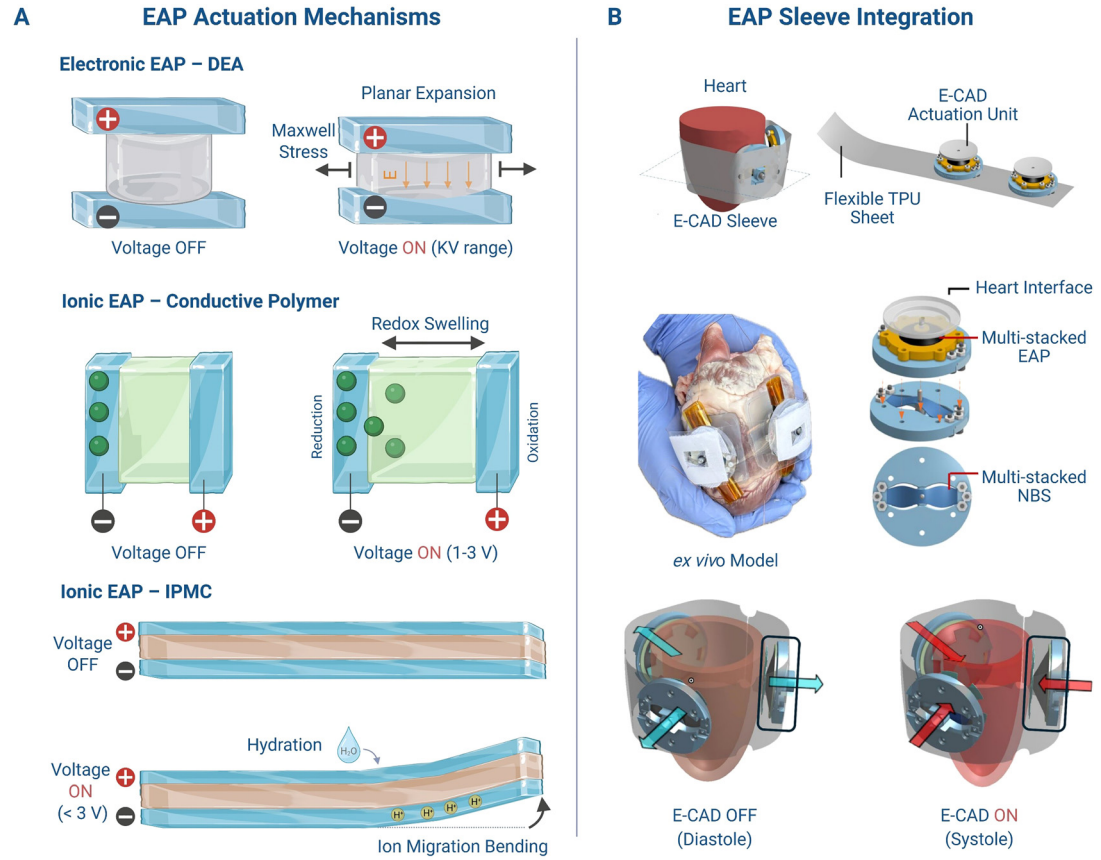

Fig. 9 Mechanisms and device integration of electroactive polymer (EAP)-based cardiac assist systems. (A) Schematic illustration of actuation mechanisms in electronic and ionic EAPs. Electronic EAP – dielectric elastomer actuator (DEA): application of a high electric field (kV range) generates Maxwell stress, resulting in thickness reduction and in-plane (planar) expansion. Ionic EAP – conductive polymer (CP): low-voltage stimulation (1–3 V) induces reversible oxidation and reduction reactions, leading to ion insertion and redox-driven volumetric swelling. Ionic EAP – ionic polymer–metal composite (IPMC): hydration-assisted cation migration (<3 V) toward the cathode produces asymmetric swelling and bending. (B) Integration of EAP actuation within an electroactive cardiac assist device (E-CAD). The multi-stacked EAP actuators are embedded within a flexible thermoplastic polyurethane (TPU) sleeve and mechanically coupled to a negative bias spring (NBS) structure. The device interfaces with the epicardial surface to provide synchronous assistance, remaining passive during diastole (E-CAD OFF) and generating circumferential compression during systole (E-CAD ON). The *ex vivo* model demonstrates sleeve conformity and actuation around the cardiac surface. Images reproduced under the terms of the CC 4.0 licence from ref. 67 E-CAD: electroactive polymer-based cardiac assist device with low power consumption, published in Advanced Intelligent Systems. Part A of figure created with https://www.Biorender.com.

lower voltage than the VAD.[79] Current-limiting circuits and mechanical insulation may be investigated to mitigate exposure to high currents in the event of device malfunction. However, long-term cyclic fatigue, electrode delamination, and dielectric breakdown under repetitive cardiac loading remain significant translational challenges for chronic implantation.

Dielectric elastomers have also found applications in augmenting the aorta in failing hearts, replacing portions of the aorta where bulky intra-aortic balloon pumps are normally used.[80,81] In one example of such an application, a DEA of four stacked elastosil films, with the upper and lower layers as passive layers for insulation, and two active inner layers with about 100 μm thickness, were glued together and embedded in a silicone casting to protect the environment from the high voltage. The device provided cardiac assistance without aortic obstruction but provided low volume change (<2 ml) and about <7 mJ in an anaesthetised acute porcine model.[80]

In another research, a tubular silicone DEA using Elastomer 2030®, was stretched prior to use and caused about 28 cm^3 displacement of fluid in the laboratory set up. As with DEA actuators, maximum contraction was observed at a high voltage 6 kV.[86]

The use of DEA in DCC offers high speed actuation, large strains, noiseless operation, and the self-sensing ability. The major limiting factor to their use as soft robotic cardiac sleeves despite their fast actuation and high strain capacity is the high operating voltage which is usually in the range of kilovolts, which can lead to a breakdown of the dielectric system itself and falls outside the desired voltage for implantable medical devices which is 2–3 V. This exceeds the typical low-voltage operating range preferred for chronically implantable cardiac systems and necessitates additional insulation and power management strategies. Other draw backs are difficulty in scaling up and the need to use stacked configurations to obtain

contraction.[74,87] Compared to pneumatic cardiac sleeves, DEA-based systems offer reduced bulk and faster electromechanical response, although at the expense of increased electrical complexity and high-voltage requirements.

While dielectric elastomers represent the most extensively studied electronic EAPs for cardiac applications, ionic electroactive polymers offer an alternative actuation mechanism that operates at substantially lower voltages.

4.2.3.1. Ionic electroactive actuators. Conductive polymers (CP) have also been studied as artificial muscles form the nineties, the polymers undergo oxidation and reduction reaction in a reversible manner to produce actuation. Conductive polymers have the characteristics of both metals and plastics. Actuation can be enhanced in some polymers by the introduction of ions, or conductive materials into the matrix of some polymers using a technique called doping. Some CPs have been used as medical implants and biological electronic devices. Examples of CPs include polypyrrole (PPy), Polyaniline (PANI), poly(3,4-ethylenedioxythiophene) poly(styrene sulphonate) (PEDOT:PSS).[88–91] The materials are less rigid than metals and biocompatible. They have been used in the tissue engineering of cardiac patches and in medical implants and have the potential to serve as biohybrid actuators that can mimic cardiac contractions in soft robotic sleeves, or as sensors for integration into such devices. Conductive polymers have also been shown to have the ability to enhance and repair electrical function in damaged cardiac tissues.[57,92,93] In addition to actuation, their inherent conductivity allows for potential integration with electrophysiological sensing and closed-loop synchronisation strategies.

Examples of previous applications in cardiac support include the triple-layered polypyrrole strips used for ionotropic support to the right ventricle of a rat model using cardiomyoplasty. The triple-layered polypyrrole sleeve produced bending actuation. With the strips around the right ventricle of a rat, electrical stimulation was carried out using AA batteries to produce systolic contraction in synchrony with native contractility.[94,95]

4.2.3.2. Ionic polymer-metal composites. Another group of electroactive polymer actuators is ionic polymer-metal composites (IPMCs). Typically made from hydrated ionic polymer membranes (nafion or flemion) coated with conductive, thin, and pliable metal electrodes like platinum or gold, they require low voltage for actuation.[77,90,96,97] An intraventricular assist device for managing cardiac failure was designed using an ionic polymer metallic composite material, perfluorosulfonic acid (PFS) membrane plated with gold/platinum. The device required less than 3 V for actuation and produced a compressing and twisting motion when actuated. The device had complementary actuators made from shape memory alloys (SMA).[90,98]

4.2.4. Shape memory alloys/polymers actuators. SMA actuators are thermal actuators which have also found wide cardiovascular applications as self-expanding stents and catheters.[99] The alloys are actuated by temperature changes to initiate dimensional changes. With more biocompatibility, the polymeric form, shape memory polymers are gradually evolving and have cardiovascular application potential. While shape memory alloys deform in response to heat, shape memory polymers are responsive to several triggers like moisture, light, heat, pressure, pH and enzyme degradation.[100] Nickel-titanium is largely resistant to corrosion, making it desirable for use in implantable devices.

As cardiac assist devices, SMA fibers were used to make an artificial myocardium device that improved myocardial contraction[101] In another research, martensitic transformation of the alloy was used to mimic heart contraction using 150 μm SMA fibres which generated force of $\approx$3.92 N.[102] Also a ventricular restraint device, made from elastic nitinol into a mesh like device, Paracor Heart Net, has been used for heart shape remodeling.[103] In making soft robotic sleeves, drawbacks of SMA actuators like hysteresis, slow deactivation and cooling, cost, and high actuation temperatures would require mitigation.

4.2.5. Peano-hasel actuators. The Peano-HASEL (hydraulically amplified self-healing electrostatic) systems are a hybrid system that combines the advantages of both hydraulic and electrostatic systems and with further refinement may serve as a template for soft robotic sleeves. They are affordable soft electrohydraulic transducers that simulate the contraction of muscles eliminating the need for rigid frames, stacked configurations or pre-stretch requirements for dielectric systems, eliminating the need for rigid frames, stacked configurations, or pre-stretching requirements typical of dielectric elastomer systems.

The system uses locally confined dielectric fluid, eliminating the need for external fluid, which also reduces the fluid travel time. A research work used rectangular pouches made from biaxial polypropylene film (BOPP) (usually used for food packaging), which are flexible but inextensible, and filled them with a liquid dielectric, Environtemp FR3, a transformer vegetable oil with high break strength. Electrostatic forces which are determined by Maxwell Pressure, cause a liquid displacement when voltage is applied to the actuators. Ionically conductive hydrogel electrodes were used for voltage production across the actuators and actuator lifecycle was about 20 000 cycles. Fast actuation and about 10% strain was observed at 10 kV with a load of about 20 g strain but as with DEAs, high voltages of around 6 kV to 10 kV were used and high voltage mitigation would be required if the actuators are to be used as soft robotic sleeve.[74]

4.2.6. Hydrogel actuators/moisture driven actuators. Hydrogel-based actuators use the ability of hydrogels to swell or shrink in response to stimuli to generate mechanical motion while moisture driven actuators can convert energy from moisture absorption into mechanical motion. A futuristic approach would be to trigger such actuation using the fluids of the human body. The hydrogel-based actuation is observed in some types of polymers that can swell when a solvent penetrates the polymer network. The swelling results in a change in mechanical properties and the creation of extra pressures when positioned in a confined space. The reverse process can occur when such a polymer loses the absorbed solvent/liquid molecules by deswelling.

Due to the limited mechanical strength of hydrogels, the incorporation of a mechanically strong component may be

helpful. Such actuators can be exemplified by multilayers of hydrogels encased in polymers, forming composites that provide actuation through volume changes resulting from hydrogel swelling and deswelling. Typically made of two parts, the host material, and the guest infiltration material. Host materials range from carbon nanotubes to cheaper materials like niobium. The volume change is driven by temperature, polar solvents, or changes in pH. They bring in an interesting perspective as the actuators can be integrated with other actuators like to electrothermal actuators to bring down operating temperatures to suitable temperatures for implantation in the body.

Water-based actuators have further evolved from guest filled systems to sheath-run systems. In sheath-run systems, the guest material is outside of the core unlike in guest-filled artificial muscles where the guest material is inside the core. Sheath-run systems have achieved better work capacity and are easier to produce. For example, the ratio of the maximum work to the contraction time work of guest-filled carbon nanotube muscles was increased by a factor of 1.7–2.15 when sheath-run muscles were actuated electrothermally or by vapor absorption. Solvent application to the surface prevents the infiltration of the guest material, the actuators made using the sheath-run technique eliminate the travel time into the core observed in guest-filled systems to obtain actuation. The system can be applied to muscle types where actuation is driven by volume expansion that results in a partial untwist in the artificial muscles occurs by partial untwist those results in torsional and tensile actuation.[104]

The integration of fluidic actuators into other actuator types can serve diverse functions. Firstly, the actuators can be incorporated to amplify the actuation properties of the original actuator, thereby resulting in lower operating temperatures or increased efficiency of the composite systems. The host provides the mechanical strength lacking in hydrogel actuators.[105]

In cardiac assist devices, moisture-driven actuators bring biocompatibility and tissue friendliness to the table and can bring down the operating temperature of current actuators that operate at higher-than-normal body temperatures.

4.2.7. Dynamic cardiomyoplasty. Dynamic cardiomyoplasty is a technique where part of the patient's own skeletal muscles are wrapped around the failing heart, and stimulated using a pacemaker technology to stimulate beating in synchrony with the native heart's contractility. The first successful cardiomyoplasty was done by Dr Carpentier in 1985 and since then the technique continues to undergo refinement, and may be worth exploring in DCCS.[106] A right ventricular support was provided using the technique alongside a triple-layered polypyrrole strip in the research work by Ruhparwar A, *et al.*[95]

Beyond direct cardiac assistance, emerging soft robotic sleeve platforms are increasingly being used as mechanobiology and disease-modeling systems to recreate pathological cardiac loading and hemodynamic environments. Recent studies have demonstrated patient-specific soft robotic models for simulating heart valve disease, aortic stenosis, ventricular remodeling, HFpEF physiology, and benchtop mitral valve testing, enabling controlled investigation of disease progression, intervention planning, and device benchmarking.[107–110] This broader perspective highlights that sleeve design can serve not only to restore failing cardiac motion, but also to intentionally perturb biomechanical environments for studying disease-relevant remodeling pathways.

4.3. Control strategies for soft robotic cardiac sleeves

Traditionally, open-loop control systems, in which a device contracts without regard for its native contractility, have limited applications. With increasing understanding of cardiac–device interaction, closed-loop systems that synchronise actuation with intrinsic cardiac activity have become the preferred strategy for direct cardiac compression systems (DCCS).

In VADs, which are mostly open-loop control, excessive pumping has been reported to cause damage to heart tissue. Inadequate or mismatched pumping rates may result in persistent heart failure symptoms. The situation occurs when continuous flow VADs have the speed set by a clinician and operate at a constant pump rate or speed, resulting in a lack of variance in cardiac parameters such as heart rate and arterial pressure that naturally vary with moods and activity levels in sleep and exercise.[111–115] These observations highlight the limitations of fixed-speed actuation in dynamic cardiovascular environments.

To overcome the drawback of the open-loop systems in DCCS, closed-loop control systems integrating ECG or other cardiac signals in precise therapy can be integrated into DCC sleeves and devices to give real-time feedback from the heart to set the parameters. Closed-loop control systems can be self-sustained or externally controlled systems. Three key components are required for real-time adaptive control of DCCS: physiological sensing of heart parameters, active compression, and data analysis.[116] Together, these elements enable synchronised and responsive mechanical support (Fig. 10B).

In closed loop systems the system senses the pressure in the ventricles collects and transmits the data to the electronic control unit that triggers compression based on received information. Wireless systems of transmission include Bluetooth technologies with low energy consumption and near field technologies, or a hybrid of both systems. These approaches offer flexibility, improved patient mobility, and reduced dependence on external hardware. Wireless technologies are rapidly evolving and can be used in DCCS control systems as they have many advantages over wired systems. Wired communication systems offer the advantage of being stable and efficient, but there are undesired effects like water damage, skin irritability, electrical appliance disruptions and infections.[116] Wireless power delivery using triboelectric nanogenerator system may be suitable for fully implanted low power consuming DCCS in the future.[67] Such developments are particularly relevant for long-term implantable systems.

There are different cardiac parameters that can be measured by sensors to provide closed-loop control systems. Signals like the pulse wave, seismocardiogram (SCG)/ballistocardiogram (BCG), electrocardiogram (ECG), phonocardiogram (PCG) and apexcardiogram (ACG) can be used in the measurement of cardiac parameters.

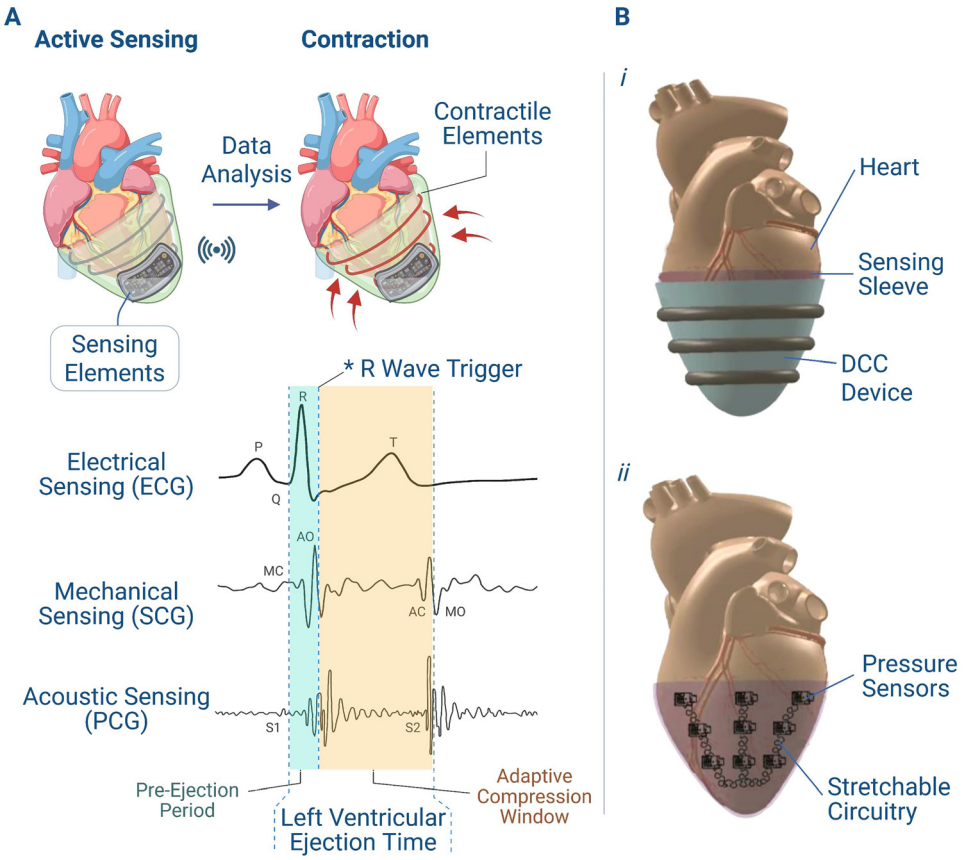

Fig. 10 Closed-loop sensing and compression strategy for direct cardiac compression systems (DCCS). (A) Schematic illustration of multimodal sensing integrated within a soft robotic cardiac sleeve. Electrical (ECG), mechanical (SCG), and acoustic (PCG) signals are analysed to define an adaptive compression window synchronised to the R-wave trigger and left ventricular ejection period. (B) Representative hardware implementation of an epicardial sensing sleeve: (i) sensing sleeve integrated with the DCC device; (ii) sensing sleeve alone, illustrating embedded MEMS barometric pressure sensors and stretchable circuitry. Images reproduced with permission from Ellen Roche and colleagues.[68] Part A of figure created with https://www.Biorender.com.

The pulse wave speed measures the arterial stiffness which can be continuously measured using photoplethysmography. SCG measures the vibrations on the chest wall caused by the mechanical activity of the heart, alongside the BCG, both measure the complicated weak force generated by the heart while pumping blood. These signals can be captured using wearable or minimally invasive sensors, making them potential candidates for long-term monitoring in DCCS applications.

ECG, which is most used, measures the electrical activity of the heart on differentiated cardiomyocytes that can conduct electrical signal. It includes the QRS and T waves that characterise the heart rhythm. Phonocardiogram measures the sounds made by the heart during contractions like the S1–S4 sounds, while ACG measures the mechanical movement of the apex of the heart *via* a pressure transducer. A combination of one or two signal measurements can be used to predict/measure cardiac parameters like the stroke volume, cardiac output or peripheral parameters like the blood pressure, and incorporated into DCCS.[117]

Sensing techniques for DCCS need to be reliable and durable for a minimum of at least 10 years. Various sensing mechanisms include the piezoelectric, piezoresistive, triboelectric, microelectromechanical systems (MEMS) and capacitive mechanisms. Techniques need to be sensitive to mechanical changes in the heart rhythms, endocardial pressure, cardiac output, or stroke volume changes, and should be capable of measuring minute changes in the deep tissues.[118]

R wave pacemaker ECG sensors have been integrated into soft robotic cardiac sleeves in the research work by[63] R-wave detection has been widely adopted as a trigger for synchronised actuation. The sensors were used to develop a synchrony between the ventricles and the pneumatic actuators. The R wave ECG detection at the beginning of systole coincides with ventricular depolarisation and serves as the trigger for actuation. The technique offers precise timing but there might be inhibition of the human heart adapting to its metabolic needs because of the pacemaker resulting in decreased contractility of the heart.[63,119]

The sensors can be placed directly on the heart or on the skin for non-invasive measuring sensors. An example of the heart surface placement is a soft robotic sleeve with embedded pressure sensing using MEMS barometric sensors, which was used in the research work.[68,120] The customised sensor, which detected heart wall deformation to guide the timing of

compression, was made from barometric sensors in a circuit embedded in a thin silicone sheet (Fig. 10B). It was tested for about 10 000 cycles and did not impede the operation of the soft robotic compression sleeve.[68]

Recently, another heart surface measurement is the pneumatic system incorporated ECG sensors for synchronisation with native contractility. Three bipolar ECG electrodes were placed within the tricushioned layers of the reBEAT device. Continuous monitoring of ECG signals was continuously detected and interpreted in real time using control algorithms to identify the R and T waves for exact epicardial compression timing.[49]

The CorInnova device also features an inbuilt sensor for native contractility sensing, the R wave is also targeted for epicardial compression timing using a cardiac trigger monitor to detect ECG using electrodes placed on the epicardium in this work,[65] the sensing electrodes are reported to be more robust than skin sensing electrodes[66] However, the drawback of using only the R wave is the atrial contribution to preload is ignored which can be captured using the P wave, and diastolic timings which can be captures using the T waves are also ignored. There may also be wrong timing of epicardial compression in patients with atrial fibrillation as other peaks like the P or T are not taken into consideration.

4.4. Structural design of DCCS

4.4.1. Configuration. The structural design of any cardiac assist device takes into cognisance the intricacies like the shape of the heart, contraction direction of native cardiac cells, individual circumstances like which of the ventricles has failed, type of heart failure, presence or absence of an enlarged heart and whether the heart requires reverse remodelling, and whether infarcted tissue is present. Therefore, geometric conformity and mechanical compatibility with the native myocardium are fundamental design considerations in DCCS.

For VADs, there is limited consideration for heart shape and cardiac mechanics as the pump takes over the pumping action from the affected ventricles, but for soft robotic devices, it is important to critically evaluate every detail to ensure efficient cardiac compression. Unlike VADs, DCCS rely on mechanical coupling with the epicardial surface and therefore must respect native myocardial kinematics.

The simplest way to design a soft robotic sleeve is using a circumferential sleeve like the CorInnova compression device. While circumferential sleeves are effective, most studies have only achieved an ejection fraction improvement of about 15–20% with that configuration. Typical example is in the CorInnova device that was shown to improve ejection fraction by 11% in this proof of concept.[66] The limitation arises from the unique configuration and shape of the human heart that utilises more than the compressive force in ejecting blood.

The normal heart is asymmetrical with roughly ellipsoid shape in the left ventricle, and a crescent shape in the right ventricle. Still, it becomes rounded to a spherical shape in failing hearts. Normal contraction occurs by both compression and twist like motions, during systole, the base of the heart rotates clockwise while the apex rotates in an anticlockwise manner producing a wringing or torsion like movement (Fig. 11).

Further explaining the twisting motion is the myocardial contractions which result in a 15–20% length contraction and 15–20% ejection fraction. The twist motion of the spherically oriented myocardial fibres ensures that an ejection fraction of up to 70% is achieved. The rotation decreases and results in reduced rotational or twist motion in some heart conditions like myocardial ischemia. Heart twist angles are measured using MRI and Doppler techniques. In heart failure patients with preserved ejection fraction where the heart fails to relax during diastole, higher values of twist rotation have been measured during diastole. The subendocardial fibres are positioned at $\approx 60^\circ$ to the long axis, while subepicardial fibres run at 60° in the opposite direction. The pericardium also contributes to the twist motion, indicating that cardiac assist devices design should aim to maintain an intact pericardium.[121]

Although twist-only external cardiac compressions have not produced superior haemodynamic outcomes compared to circumferential models, hybrid compression–torsion models have demonstrated improved performance. As seen in the soft robotic sleeve by,[63] which took into cognisance both the compressive and twist heart motions by designing two layers of actuators based on a 3D heart model and the bilayer actuator model restored 88% cardiac output in a porcine model. The soft robotic device by[73] also accounted for both compressive and twist forces.

Both works emphasise the need for individual customisation of the device based on heart imaging rather than imposition of pre-thought models to optimise mechanical action. Individual customisation would reduce risks of myocardial ischaemia or contusions. Designed models should also take into consideration ways to prevent damage to the coronary arteries. Finite element modelling and patient-specific computational simulations are increasingly used to predict stress distribution, epicardial shear forces, and regional deformation prior to implantation, thereby reducing mechanical mismatch and localised tissue injury.

4.4.2. Technical force requirements. Though an average of about 390 N is used during CPR to provide effective pumping, placing a device directly around the heart is more effective and requires lower force. It is important to note that CPR represents external thoracic compression, whereas DCCS provide direct epicardial compression, resulting in different mechanical transmission efficiencies.

A systolic pressure of about 140 mmHg is 18.5 kPa (1 mmHg is $\approx$0.13 kPa which is 133 N m^{-2}). Assuming the human heart is symmetrical and spherical in shape, a hemispherical or cup-shaped DCC device placed around the typical male heart that is about 13 cm diameter, a force of about 60 N would be required for total pumping using an idealised model formula in the research work by[122] the formula depicts the tension or force requirement for a hemispheroidal DCC device to generate meaningful contraction as a product of the assisted pressure to the heart and the cross-sectional area of the device, divided by two.[123]

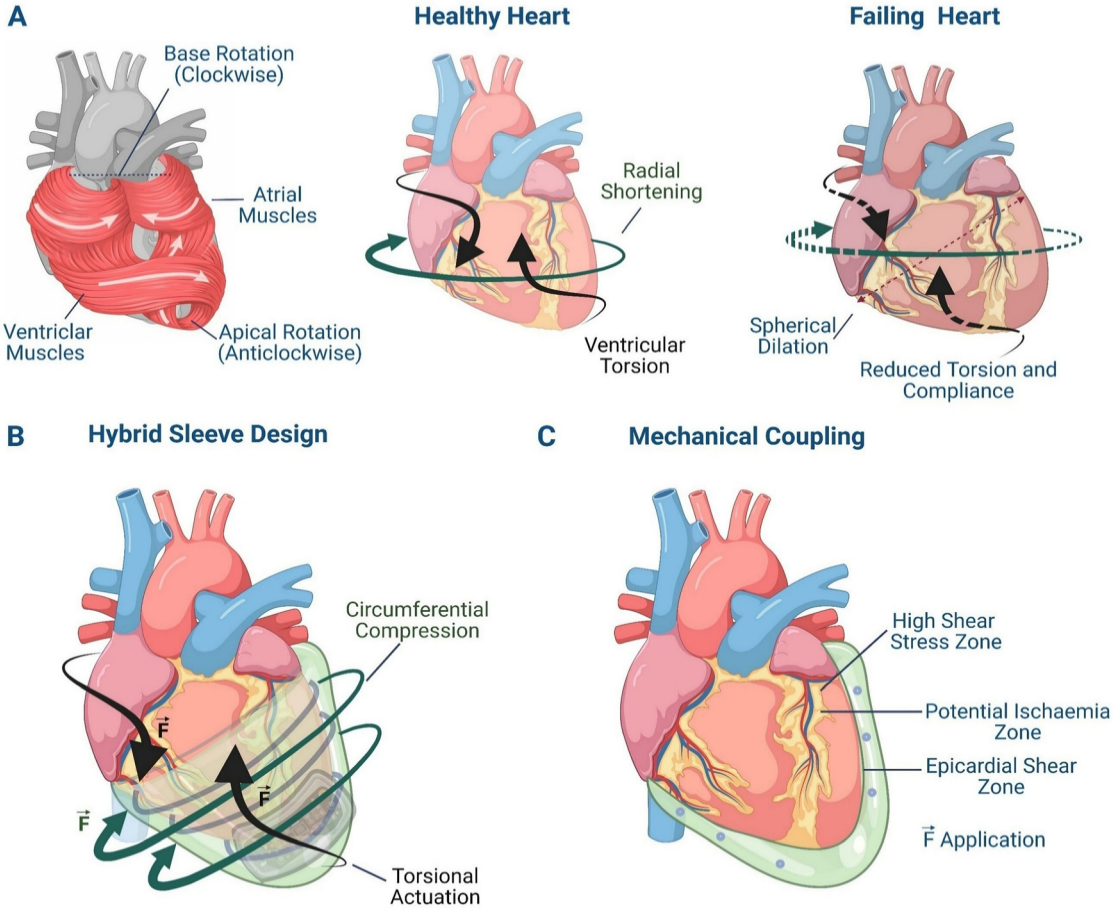

Fig. 11 Structural and biomechanical considerations for hybrid direct cardiac compression systems (DCCS). (A) Native ventricular mechanics illustrating preserved ellipsoidal geometry, radial shortening, and physiological torsion generated by opposite rotations of the base (clockwise) and apex (anticlockwise). In failing hearts, spherical remodelling is associated with reduced torsion and diminished compliance. (B) Hybrid sleeve configuration integrating circumferential compression with torsional actuation to replicate native wringing motion and improve mechanical efficiency. (C) Mechanical coupling between the epicardial sleeve and myocardium, highlighting force distribution and potential high shear stress regions that may predispose to epicardial injury or localised ischaemia if not appropriately optimised. Figure created with https://www.Biorender.com.

Although simplified spherical assumptions are useful for force estimation, the anisotropic geometry and heterogeneous stiffness of failing ventricles introduce spatially varying stress distributions that may alter actual force requirements. Since the heart has some residual contractility with a failed heart showing an ejection fraction of $<40\%$, typically, having systolic pressure less than or around 90 mmHg, a 50 mmHg pressure boost is 6.7 kPa, which is 0.6 N cm^{-2}, reducing the required force to a range of 10 – 60 N as required. A pneumatic system with force of 10 N producing about 20 mm Hg assistance and an increased ejection fraction in sheep model.[124]

Also in a previous review by Howarth *et al.*, the importance of both force and positional placement of DCC were emphasised, another factor to consider in the increased stiffness in infarcted or failing hearts, which may increase the force requirements.[119] Additionally, excessive compressive force may elevate epicardial shear stress and compromise coronary perfusion, highlighting the need for balanced mechanical assistance.

For individual artificial muscles, an output strain of up to 20%, and a maximal strain of about 80% operation bandwidth of <10 Hz, work generation of about 1 Joule per heartbeat, and an efficiency of about 25% would demonstrate a potential DCC actuator.[59]

In essence, proper designing takes into cognisance patient-specific factors while optimising the actuator systems as well.

4.4.3. Durability. While designing DCCS, the durability of the actuators should also be factored in so that the actuators are durable, not prone to degradation, and able to go for billions of cycles bearing in mind that the human heart muscles are not prone to fatigue and are able to contract up to 100 000 times in a day. Their durability also serves to prevent the need for replacement or repeated surgeries. The reBEAT has been shown to have some durability with the device being able to go up to 80 million cycles.[49]

However, long-term durability assessment must also consider material fatigue, creep behaviour, hydrogel dehydration, dielectric breakdown (for EAP systems), and hysteresis-related

degradation (for SMA-based systems). Chronic implantation requires stability over billions of cycles, corresponding to multiple years of continuous cardiac support. Accelerated life testing and *in vitro* cyclic fatigue protocols are therefore essential to predict actuator longevity under physiological loading conditions.

4.4.4. Implantation/Fixation. The implantation/fixation techniques of a DCCS to the human heart are another crucial part of the design process. VADs are typically implanted by median sternotomy which is a largely invasive procedure taking up to 8 hours surgery time. This has resulted in some considerations being given to lateral thoracotomy or hemi sternotomy for VADs in a bid to reduce the invasiveness. The parts of a VAD that are surgically fixed include the inflow canula, housing of the pump, outflow graft and the driveline. The disadvantages of largely invasive implantation procedures include surgical trauma, higher risk of perioperative bleeding, increased risk of right ventricular failure with the full opening of the pericardium, complications in wound site healing, increased chest instability risk leading to higher risks of infection and greater chances of readmission.[125,126]

DCCS has shown potential for less invasive implantation as collapsible devices requiring smaller surgical cuts have been designed. Examples are the CorInnova and the reBEAT devices. The CorInnova device is implanted by mini left thoracotomy to access the heart apex and can be implanted in minutes. The reBEAT which has also been reported to be implanted in minutes *via* a miniaturised partial sternotomy.[64,127]

For fixation, an issue for DCCS is how to secure the device to the apex and base of the heart, and to the moving myocardium, to ensure maximal adhesion and efficient coupling while minimising tissue damage. The use of adhesive or suction has been studied for apical integration, and a combination of Velcro and suturing was found to be most effective, and for attachment to the myocardium, the medical mesh integrated nicely and proved superior to silicone implants for myocardial integration.[128]

In addition, long-term epicardial integration must consider fibrosis formation, pericardial adhesion, and potential interference with coronary arteries. Secure fixation should allow sufficient mechanical coupling without inducing ischaemia or impairing physiological myocardial motion.

The effectiveness of sleeve-based support also depends critically on epicardial coupling mechanics and force transmission efficiency. Previous passive ventricular constraint studies demonstrated that distributed epicardial loading can significantly influence reverse remodeling outcomes.[129] Conversely, poorly synchronised or non-physiological actuation patterns may adversely alter ventricular pressure–volume relationships, reduce energetic efficiency, and compromise the reverse remodeling benefits of external support.[130,131] These considerations further emphasise the importance of anatomically informed sleeve architectures and synchronised control strategies.

4.5. Preclinical demonstrations

With the advent of time and technology refinement, soft robotic sleeves are typically moving from laboratory silicone test models to *ex vivo*, then animal models and more recently human trials. Devices have been tried in different animal models (Table 1): sheep,[58] canines,[70] calves,[72] goats[58,132] and pigs[49,133] Beta blockers like esmolol are commonly used to induce heart failure and reduce ejection fraction. The use of esmolol has the advantage of low cost, low animal mortality and fewer cases of arrythmias, it may however cause a low preload resulting from dilation of the great vessels.,[65] although it may cause reduced preload secondary to dilation of the great vessels.

The anstadt cup was first tested in humans in the 1960s, where it was used for one hour resuscitation. It was tested under the name DMVA (Direct Mechanical Ventricular Actuation), and in the 90s, the device was tested in about 22 patients who had refractory cardiac arrest and were aged $\approx$45 years, including male and female. Implantation took about 2 minutes, and an average of 78 and 41 mmHg, systolic and diastolic blood pressure, with average cardiac output of about 3.14 litres/min measured in the patients. No damage to the heart from the device was reported.[58,134] The first attempt to use a DCC device to manage heart failure was carried out using the Heart Booster (AbioBooster), on a calf model, and the device resulted in a 10% cardiac output increase, and 15 mmg Hg pressure increase. More recently, modern direct compression systems have progressed beyond acute animal validation towards early human feasibility studies.

The ReBeat and CorInnova pneumatic devices have been put through animal trials successfully and are progressing to human trials. For the reBEAT, in a human experience, the device operated for about 45 minutes where it was implanted in a patient due to receive an LVAD. Implantation on the beating heart was fast, taking a few minutes, with immediate confirmation of six-channel ECG detection enabling synchronisation with the native rhythm while providing pneumatic augmentation. A 12% increase in cardiac power output was reported in six patients. The device has also demonstrated diastolic correction of the T-wave deflation timing, with approximately -50 ms adjustment observed in an animal model. The CorInnova device is set for first-in-human use soon.[64,127]

4.6. Challenges and limitations

The tremendous progress achieved by DCC devices in providing external mechanical compression to the heart is huge, largely eliminating many of the concerns and untoward effects of rigid VAD systems (Fig. 12). From cost to limited blood contact, noiseless operations, minimal invasiveness, and portability, to mention a few. Nevertheless, there remains a long way to go in achieving seamless integration with failing hearts.

4.6.1. Mechanical durability and long-term reliability. The first major challenge on the long term is producing a reliable, precise actuation system that is reproducible and durable for billions of cycles. Currently, most soft robotic devices have been tested only in acute failure, asides a few devices like the CorInnova which has been tested in

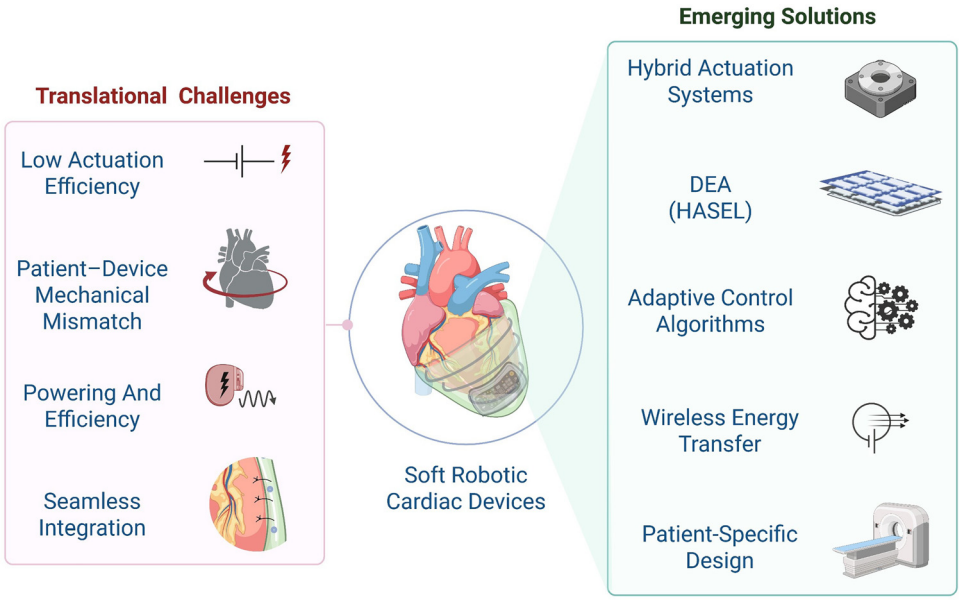

Fig. 12 Translational challenges and emerging technological solutions for soft robotic cardiac compression devices. Current limitations in direct cardiac compression systems include low actuation efficiency, patient–device mechanical mismatch, limitations in powering strategies, and difficulties in seamless integration with the cardiac environment. Emerging approaches aimed at overcoming these barriers include hybrid actuation systems, dielectric elastomer actuators (DEAs) such as HASEL actuators, adaptive control algorithms for synchronised actuation, wireless energy transfer strategies, and patient-specific device design.

animal model for up to 14 days and is being proposed for up to 7 days use as bridge to transplantation. The reBEAT device has been tested for up to 30 days in porcine model with success, and the heart patch tested for 7 days. Future systems must demonstrate durability approaching current-generation VADs such as the HeartMate 3, which can function for five years or more.

4.6.2. Energy efficiency and power management. The second major challenge is the efficiency of the actuating systems. Currently, the most efficient VADs have an efficiency of about 25% and sadly, proposed soft robotic sleeves are not any better. An efficient actuation would improve the quality of life of patients by decreasing the charging frequency and limit heat generation where applicable.

4.6.3. Biomechanical modelling and patient-specific force requirements. A third challenge is the lack of robust data on torsional displacements, mechanical data and forces required to produce desired ejection fraction in failing hearts, prevent wall stresses and help improve heart muscles where there is remodelling.[8,135] Though some force requirements are documented in these reviews.[59,136] comprehensive population-scale datasets derived from CT and MRI imaging remain limited. There is still room for modelling and proposing the required force based on studies of a significant number of images from CT and MRI scans representing a typical failing heart, capturing the residual pumping activity, directions of contractions in the presence of infarcts, to obtain a relevant range of data that are able to depict the population. An established dataset can be used in actuator design, allowing for individual heart customisation.

Closely related to this challenge is the intrinsic asymmetry of the human heart and heterogeneous ventricular wall thickness, which complicate actuator architecture. Examination of symmetric *versus* asymmetric compression strategies is therefore critical. While circumferential models have improved ejection fraction, twist-only models have produced less than desired augmentation. Importantly, synergy between twist and circumferential compression, with circumferential elements positioned externally, produced the best cardiac output in reported work.[63] Consideration must also be given to interventricular septal positioning following implantation, as current single-ventricle support systems may disrupt contralateral ventricular function.[137]

4.6.4. Material selection, fixation and surgical integration. Another precaution is the careful choice of materials to prevent cardiac contusion during long-term use. Devices must achieve effective epicardial compression without inducing inflammation, myocardial bruising, ventricular inversion, or diastolic restriction. Earlier models such as the anstadt cup caused ventricular inversion because of rigid framing; newer devices such as CorInnova use superelastic nitinol frameworks to mitigate this risk.[58,64,66]

Fixation strategies are equally critical. Suturing remains common, although CorInnova and reBEAT employ self-deployment mechanisms that reduce the need for full sternotomy and decrease invasiveness. Devices implantable *via* mini-thoracotomy approaches may reduce infection risk and recovery time. Preservation of the pericardial sac is also important, as it plays an active role in native myocardial mechanics. In patients with compromised pericardium, fixation may present additional challenges.

5. Emerging trends and future directions

The continued development of DCC technologies depends on addressing several key translational challenges, including actuator efficiency, device–tissue mechanical compatibility, power delivery, and long-term integration with the cardiac environment. Advances in soft robotics, materials science, and biomedical engineering are beginning to offer promising strategies to overcome these barriers. In particular, emerging research is focusing on improved actuation strategies, intelligent control systems capable of synchronising with native cardiac mechanics, and patient-specific device architectures that enhance mechanical compatibility and clinical adaptability. The following subsections discuss these emerging directions and their potential to advance soft robotic cardiac compression devices toward clinically viable mechanical cardiac support systems (Fig. 12).

5.1. Hybrid technologies

As technological advancements in soft robotics continue, the miniaturisation of currently bulky pneumatic systems represents a highly desirable development for DCC. The substitution of pneumatic actuators with smaller hydraulic systems, or other actuator systems such as twisted and coiled polymer actuators and improved dielectric elastomer actuators (DEAs) such as Peano-HASEL or donut-shaped HASEL actuators, can lead to the development of miniaturised and truly portable devices.[138]

Better still, a hybrid system utilising more than one actuation mechanism may optimise the advantages of each individual system. A good example is a guest–host composite system, where the guest may be a gel, wax or polyethylene glycol, and the infiltrated host could be carbon nanotubes, twisted and coiled polymers, or elastomeric materials such as silicone rubber. The composite system acts like a hygromorphic artificial muscle, where volume change drives dimensional changes that can result in muscle length contraction, increase in diameter, and fibre untwist. The guest layer can contribute to torsional actuation through swelling and deswelling while lowering the operating temperature.

For example, the addition of a thermosensitive gel layer that undergoes a solution–gel transition with small temperature changes due to shifts in hydrophilicity/hydrophobicity, when integrated with twisted and coiled polymer actuators, may reduce the typical operating temperature ($\approx$65–80 °C). Since torsional untwisting drives actuation, the additional layer can further contribute to untwist and enhance actuation performance. Examples of guest materials in the literature include paraffin wax, PNIPAM and polar solvents. Other tuneable polymers such as POEGMA could also be considered. A successful hybrid system example is the silicone rubber/carbon nanotube fibre system, where actuation was generated *via* chemical rubber swelling in non-polar solvents without temperature change. The composites produced theoretical efficiencies of up to 16%, approximately 50% contraction, and 1.2 kJ kg^{-1} work density.[139–142] The hybrid actuator system can be tailored to produce efficient cardiac sleeves.

Another interesting group of hybrid actuators is liquid crystal elastomers, a hybrid of anisotropic liquid crystal molecules and polymeric elastomers that produce stimuli-sensitive actuators which are soft, pliable, responsive, fast, lightweight and tuneable to obtain desirable properties. Furthermore, hydrogels can be layered onto them based on intended design. This rapidly evolving class of materials warrants further investigation for application in soft robotic cardiac sleeves.[143–146]

Yet another angle is the hybridisation of current pump models and soft robotic devices. The latest HeartMate 3 has been covered with pliant materials to improve tissue compatibility. A classic example is a dielectric elastomer-based electropneumatic device. In a bid to combat the thrombotic side effects of traditional VADs, the hybrid device was made from thin silicone elastomeric film cast on compliant electrodes, which worked by voltage-induced pneumatic contractions and generated pulsatile contractions. The device, called Soft Beats, was portable, fast, weighed less than 200 grams, used approximately 0.8–1.6 watts (comparable to the 0.5–1 watt used by the native heart), and did not generate excessive heat like conventional VADs. The major drawback, as with dielectric elastomers, was the high voltage required (9–12 kV).[79]

The introduction of cells onto the surface of soft robotic devices is another area of exploration. Though soft robotic sleeves are not prone to causing thrombosis, the seeding of an endothelial cell layer on the surface of the device may further enhance biointegration and tissue compatibility.[137,147]

5.2. Biomimetic/adaptive control algorithms

The future soft robotic cardiac device will ideally be adaptive rather than operating on fixed control systems, and capable of responding to patient-specific physiological variations in preload, afterload and heart rate, such as during exercise, sleep, or Valsalva manoeuvres. This would represent a major advantage over continuous-flow VADs, which are inherently limited in accommodating dynamic physiological changes.[137]

The use of TET to support fully implantable devices, similar to cochlear implants, represents an emerging technology that could significantly improve the quality of life of patients supported by mechanical circulatory support systems. Currently, battery packs last approximately 12 hours and are carried externally along with the control pack. The need to carry battery packs can be uncomfortable for patients, and may impose lifestyle limitations, such as protective measures during showering. In addition to discomfort, driveline infections that may lead to hospital readmission remain a significant concern.[137]

Despite these challenges, recent advances in battery technology have produced promising results. TET devices operate using magnetic induction. A notable example is Coplanar Energy Transfer (CET) (Fig. 11), which addressed some limitations of conventional TET by being less sensitive to patient movement. The Leviticus Cardio system from Petach Tikva, Israel, is a CET-based device that enabled full implantation of a Jarvik LVAD for approximately two months while awaiting heart transplantation in one of two patients. The device used a coplanar energy transfer system consisting of two sizeable rings

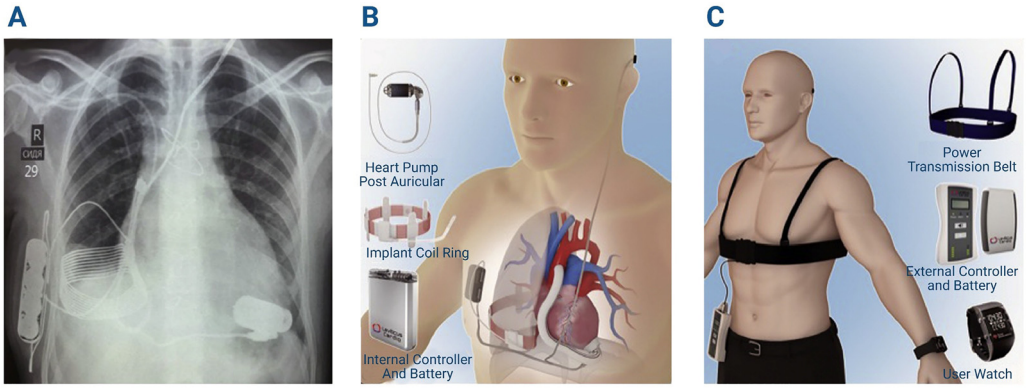

Fig. 13 Image showing (A) X-ray of implanted components (B) implanted components (C) external components of the fully implantable LVAD using the Levticus Cardio CET system for VAD powering. Reprinted from First human use of a wireless coplanar energy transfer coupled with a continuous flow left ventricular assist device. 38(4), 339–343 in J Heart Lung Transplant by[148] © 2025 with permission from Elsevier.

configured in a coil-within-coil topology. The implanted coil ring (Fig. 13) was positioned around the pleural cavity. One patient had the device explanted after 35 days due to LVAD-associated thrombosis. The younger patient reportedly engaged in activities such as swimming and had the device removed without complications.[148]

Innovative wireless technologies such as the Leviticus Cardio system may, with further refinement, be adapted to support fully implantable soft robotic cardiac compression devices.

5.3. Patient specific designs

Soft direct compression devices customised to suit patient-specific anatomy, physiology and pre-existing conditions, guided by advanced imaging techniques and virtual surgical planning, are compelling and desirable. Such approaches may reduce implantation time and minimise postoperative complications. Another important research direction involves developing laboratory models that accurately replicate human cardiac mechanics for preclinical testing. Well-designed testing platforms may enable optimisation of device architecture prior to animal studies, potentially reducing animal usage and improving translational predictability.

6. Clinical translational roadmap

Clinical translation refers to the progression of a technology from conceptual development to routine clinical application, encompassing idea generation, design, preclinical testing, clinical trials, regulatory approval, practice guidelines, physician adoption, and eventual patient use. Each stage requires multidisciplinary collaboration among engineers, clinicians, regulatory specialists, and industry partners. In the development of soft robotic devices for DCC, some systems such as reBEAT and CorInnova are approaching early clinical feasibility stages within this translational pathway. Early integration of structured risk assessment frameworks, including failure mode and effects analysis (FMEA) and redundancy planning, is essential to ensure mechanical and patient safety in active implantable compression systems.

For clarity, the translational roadmap of soft robotic cardiac compression devices can be broadly divided into three phases: (i) concept and technical development, (ii) preclinical validation, and (iii) clinical and regulatory translation.

6.1. Concept and technical development

During the concept stage, the viability of the proposed idea is evaluated against key criteria, including originality, patentability, the ability to address an unmet clinical need, feasibility for clinical implementation, cost-effectiveness, and comparative effectiveness. For soft robotic cardiac sleeves, this phase includes actuator selection, material optimisation, structural design, and preliminary laboratory characterisation. Comparative effectiveness may be assessed through the device's ability to enhance ejection fraction and cardiac output relative to existing therapies.

Once a structurally robust soft robotic configuration demonstrating desirable features such as rapid and repeatable actuation, mechanical stability, and sensor integration is achieved, intellectual property protection may be pursued. Bench testing using silicone heart models or reproducible mechanical test platforms is then performed to quantify force generation, pressure development, and repeatability under controlled conditions. Consideration of scalable manufacturing strategies, material reproducibility, and compliance with Good Manufacturing Practice (GMP) standards should also begin at this stage to facilitate eventual clinical translation.

6.2. Preclinical validation

Preclinical testing includes the use of bench models, *ex vivo* systems, and animal models to evaluate haemodynamic performance, including improvements in ejection fraction and cardiac output. A critical consideration at this stage is the selection of an appropriate animal model aligned with the intended clinical application. For devices requiring septal access, canine models are often preferred due to anatomical similarities, whereas pigs and sheep are commonly selected for infarct models because of their limited collateral circulation.

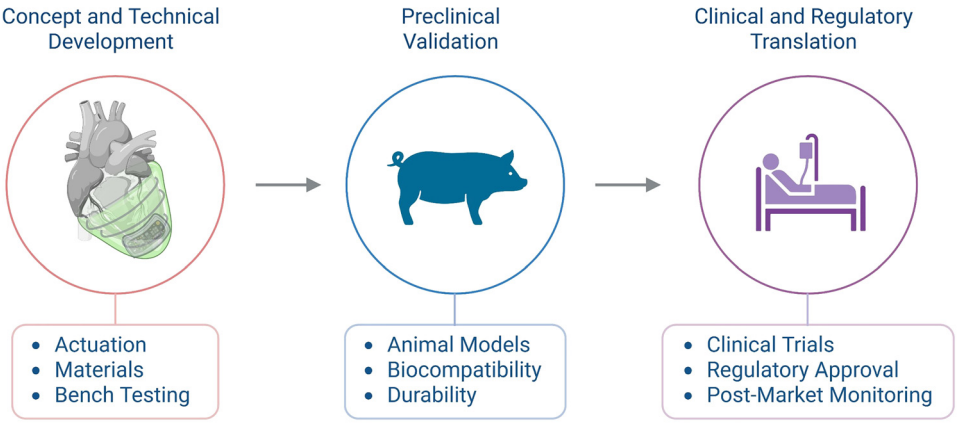

Fig. 14 Translational pathway for soft robotic cardiac compression devices. Development of direct cardiac compression technologies progresses through sequential stages from concept and technical development to preclinical validation and ultimately clinical and regulatory translation. Early-stage development focuses on actuator design, material optimisation, and bench-top testing. Preclinical validation evaluates device performance in animal models, including assessments of biocompatibility and long-term durability. Successful systems may then advance to clinical trials, regulatory approval processes, and post-market monitoring, forming the pathway toward clinically viable mechanical cardiac support technologies.

After obtaining the necessary ethical approvals, preclinical studies should be designed around clearly defined research questions understood by all members of the research team. Animal proof-of-concept studies must closely mimic anticipated human applications and rigorously assess pathological responses, tissue interactions, and physiological parameters. Inadequate preclinical validation may result in significant financial cost, time delays, and translational setbacks.

For soft robotic compression systems, animal testing also enables evaluation of overall physiological impact and early identification of potential adverse events, including device–tissue interface complications or thrombotic sequelae. Such studies may reveal technical limitations requiring optimisation prior to clinical progression, including issues related to residual myocardial activity, fixation stability, or biocompatibility.[149]

Depending on the intended indication (bridge to transplantation or destination therapy) long-term durability studies may be required to assess mechanical reliability and late complications. Notably, approximately 55% of complications associated with mechanical circulatory support devices arise from the device–organ interface following implantation.[58] Accordingly, sterilisation compatibility, long-term material fatigue, and stability within biological environments must be systematically evaluated prior to human implantation. Examples of proof-of-concept studies of soft robotic cardiac compression devices are summarised in Table 1.

Following successful preclinical validation, devices may proceed to human clinical trials after obtaining regulatory and institutional ethics approvals and informed patient consent. At this stage, regulatory classification, safety profiling, and risk mitigation strategies become critical considerations. For implantable cardiac devices, alignment with stringent regulatory pathways (*e.g.*, Class III medical device frameworks) is essential to ensure safety and long-term clinical viability.

Successful completion of early-phase clinical trials may lead to broader clinical evaluation, incorporation into practice guidelines, and eventual adoption into routine clinical care. Post-market surveillance, registry-based outcome tracking, and iterative design refinement are critical components of sustainable clinical adoption for implantable cardiac technologies. The ultimate success of soft robotic cardiac compression systems will depend not only on haemodynamic performance but also on durable biointegration, long-term safety, regulatory compliance, and clinician acceptance (Fig. 14).

7. Conclusion and future outlook

DCC has evolved from resuscitative applications to providing mechanical cardiac support over the past five decades. With continued advancements and technical refinement, DCC devices have demonstrated short-term efficacy in supporting failing hearts while mitigating several limitations associated with VADs, including thrombosis. Additional advantages include reduced device profile, synchronisation with native myocardial contractility, and limited tissue trauma. A further promising attribute is the potential for minimally invasive implantation and fixation. As device architectures continue to mature, their long-term capacity to match or surpass conventional rotary VADs in durability, haemodynamic performance, and patient quality of life remains an important translational objective.

Future development efforts should prioritise the following areas:

- Extending actuator durability to withstand billions of physiologically relevant contraction cycles under chronic loading conditions
- Advancing fully implantable and wirelessly powered system architectures
- Developing standardised, physiologically representative bench models to optimise device design prior to animal testing
- Engineering hybrid actuation platforms that integrate complementary mechanisms to overcome individual actuator

limitations, such as the high voltage requirements of dielectric elastomers, elevated operating temperatures of twisted and coiled polymer muscles, and the bulkiness of pneumatic systems

Beyond mechanical optimisation, sustained progress will depend on integrated advances in material stability, biointerface engineering, adaptive control systems, and regulatory alignment. From this translational perspective, the commercial readiness of current actuator materials is beginning to diverge across platforms. Pneumatic elastomeric systems based on silicone and thin-film TPU currently appear the most clinically mature, owing to their high force output, established manufacturability, and the strongest *in vivo* and early human feasibility evidence. Platforms such as CorInnova and reBEAT highlight the near-term commercial promise of soft pneumatic sleeves through minimally invasive deployment, durable cyclic performance, and clinically relevant biventricular support. By comparison, electroactive polymers, twisted-and-coiled muscles, and shape-memory systems remain highly promising for future miniaturised implantable generations, but still require further advances in long-term durability, thermal management, and low-voltage operation before widespread clinical translation.

Looking ahead, the role of soft robotic cardiac sleeves may extend beyond therapy into mechanobiology-driven disease simulation and preclinical testing environments, opening new translational opportunities across cardiovascular research and device development.

Conflicts of interest

There are no conflicts of interest to declare.

Data availability

No new data were generated or analysed in this study. All information discussed in this review is derived from previously published sources cited in the article.

Acknowledgements

This work was supported in part by the NSW Health Cardiovascular Senior and Early-Mid Career Researcher Grant (2024) and the NSW Health Cardiovascular Collaborative Grant Program (2025), Australia, awarded to Javad Foroughi.

References

1 B. Chong, J. Jayabaskaran, S. M. Jauhari, S. P. Chan, R. Goh, M. T. W. Kueh, H. Li, Y. H. Chin, G. Kong and V. V. Anand, *Eur. J. Prev. Cardiol.*, 2025, **32**, 1001–1015.

2 B. Chong, J. Jayabaskaran, S. M. Jauhari, S. P. Chan, R. Goh, M. T. W. Kueh, H. Li, Y. H. Chin, G. Kong, V. V. Anand, J. W. Wang, M. Muthiah, V. Jain, A. Mehta, S. L. Lim, R. Foo, G. A. Figtree, S. J. Nicholls, M. A. Mamas, J. L. Januzzi, N. W. S. Chew, A. M. Richards and M. Y. Chan, *Eur. J. Prev. Cardiol.*, 2025, **32**, 1001–1015.

3 G. Savarese, P. M. Becher, L. H. Lund, P. Seferovic, G. M. C. Rosano and A. J. S. Coats, *Cardiovasc. Res.*, 2022, **118**, 3272–3287.

4 G. A. Roth, G. A. Mensah, C. O. Johnson, G. Addolorato, E. Ammirati, L. M. Baddour, N. C. Barengo, A. Z. Beaton, E. J. Benjamin, C. P. Benziger, A. Bonny, M. Brauer, M. Brodmann, T. J. Cahill, J. Carapetis, A. L. Catapano, S. S. Chugh, L. T. Cooper, J. Coresh, M. Criqui, N. DeCleene, K. A. Eagle, S. Emmons-Bell, V. L. Feigin, J. Fernandez-Sola, G. Fowkes, E. Gakidou, S. M. Grundy, F. J. He, G. Howard, F. Hu, L. Inker, G. Karthikeyan, N. Kassebaum, W. Koroshetz, C. Lavie, D. Lloyd-Jones, H. S. Lu, A. Mirijello, A. M. Temesgen, A. Mokdad, A. E. Moran, P. Muntner, J. Narula, B. Neal, M. Ntsekhe, G. Moraes de Oliveira, C. Otto, M. Owolabi, M. Pratt, S. Rajagopalan, M. Reitsma, A. L. P. Ribeiro, N. Rigotti, A. Rodgers, C. Sable, S. Shakil, K. Sliwa-Hahnle, B. Stark, J. Sundstrom, P. Timpel, I. M. Tleyjeh, M. Valgimigli, T. Vos, P. K. Whelton, M. Yacoub, L. Zuhlke, C. Murray, V. Fuster and G.-N.-J. G. B. o C. D. W. Group, *J. Am. Coll. Cardiol.*, 2020, **76**, 2982–3021.

5 M. Cameli, M. C. Pastore, A. Campora, M. Lisi and G. E. Mandoli, *Front. Cardiovasc. Med.*, 2022, **9**, 1001002.

6 L. Miller, E. Birks, M. Guglin, H. Lamba and O. Frazier, *Circ. Res.*, 2019, **124**, 1658–1678.

7 M. S. Parmacek and J. A. Epstein, *N. Engl. J. Med.*, 2009, **361**, 86–88.

8 E. Aranda-Michel, L. K. Waldman and D. R. Trumble, *PLoS One*, 2019, **14**, e0224475.

9 E. Beslika, A. Leite-Moreira, L. J. De Windt and P. A. da Costa Martins, *Cardiovasc. Res.*, 2024, **120**, 461–475.

10 N. Hersch, B. Wolters, G. Dreissen, R. Springer, N. Kirchgessner, R. Merkel and B. Hoffmann, *Biol. Open*, 2013, **2**, 351–361.

11 Z. W. Tao, M. Mohamed, J. G. Jacot and R. K. Birla, *ASAIO J.*, 2018, **64**, e105–e114.

12 M. Litvinukova, C. Talavera-Lopez, H. Maatz, D. Reichart, C. L. Worth, E. L. Lindberg, M. Kanda, K. Polanski, M. Heinig, M. Lee, E. R. Nadelmann, K. Roberts, L. Tuck, E. S. Fasouli, D. M. DeLaughter, B. McDonough, H. Wakimoto, J. M. Gorham, S. Samari, K. T. Mahbubani, K. Saeb-Parsy, G. Patone, J. J. Boyle, H. Zhang, H. Zhang, A. Viveiros, G. Y. Oudit, O. A. Bayraktar, J. G. Seidman, C. E. Seidman, M. Noseda, N. Hubner and S. A. Teichmann, *Nature*, 2020, **588**, 466–472.

13 N. Tueni, J.-M. Allain and M. Genet, *J. Mech. Behav. Biomed. Mater.*, 2023, **138**, 105600.

14 D. D. Streeter Jr, H. M. Spotnitz, D. P. Patel, J. Ross Jr and E. H. Sonnenblick, *Circ. Res.*, 1969, **24**, 339–347.

15 P. P. Sengupta, V. K. Krishnamoorthy, J. Korinek, J. Narula, M. A. Vannan, S. J. Lester, J. A. Tajik, J. B. Seward, B. K. Khandheria and M. Belohlavek, *J. Am. Soc. Echocardiogr.*, 2007, **20**, 539–551.

16 P. Camelliti, C. Green and P. Kohl, *Adv. Cardiol.*, 2006, **42**, 132.
17 J. Baum and H. S. Duffy, *J. Cardiovasc. Pharmacol.*, 2011, 57.
18 R. Wu, F. Ma, A. Tosevska, C. Farrell, M. Pellegrini and A. Deb, *JCI Insight*, 2020, 5.
19 C. Tschöpe, B. Kherad, O. Klein, A. Lipp, F. Blaschke, D. Gutterman, D. Burkhoff, N. Hamdani, F. Spillmann and S. Van Linthout, *Eur. J. Heart Failure*, 2019, **21**, 14–22.
20 T. G. Martin, V. D. Myers, P. Dubey, S. Dubey, E. Perez, C. S. Moravec, M. S. Willis, A. M. Feldman and J. A. Kirk, *Nat. Commun.*, 2021, **12**, 2942.
21 G. Buckberg, J. I. Hoffman, A. Mahajan, S. Saleh and C. Coghlan, *Circulation*, 2008, **118**, 2571–2587.
22 P. T. Phan, J. Davies, T. T. Hoang, M. T. Thai, C. C. Nguyen, A. Ji, K. Zhu, B. Sharma, E. Nicotra, C. Hayward, H.-P. Phan, N. H. Lovell and T. N. Do, *Adv. Intell. Syst.*, 2023, **6**, 2300464.
23 S. Khan and W. Jehangir, *Cardiol. Res.*, 2014, **5**, 121–125.
24 J. A. Cook, K. B. Shah, M. A. Quader, R. H. Cooke, V. Kasirajan, K. K. Rao, M. C. Smallfield, I. Tchoukina and D. G. Tang, *J. Thorac. Dis.*, 2015, **7**, 2172–2180.
25 D. A. Cooley, D. Liotta and B. J. Messmer, *Adv. Biomed. Eng. Med. Phys.*, 1971, **2**, 47–93.
26 K. L. Baughman and J. A. Jarcho, *N. Engl. J. Med.*, 2007, **357**, 846–849.
27 Liota-Cooley Heart, https://americanhistory.si.edu/collections/object/nmah_688682 (accessed 23/09/2025, 2025.).
28 S. M. Group, *Circa*, 1980, 2017, 110 mm × 210 mm × 110 mm.
29 A. K. Puppala, V. Sonnati and S. Gangapuram, *J. Phys.: Conf. Ser.*, 2020, 1495.
30 J. Han and D. R. Trumble, *Bioengineering*, 2019, 6.
31 J. J. Han, M. A. Acker and P. Atluri, *Circulation*, 2018, **138**, 2841–2851.
32 D. Mancini and P. C. Colombo, *J. Am. Coll. Cardiol.*, 2015, **65**, 2542–2555.
33 O. H. Frazier, R. M. Delgado, B. Kar, V. Patel, I. D. Gregoric and T. J. Myers, *Tex. Heart Inst. J.*, 2004, **31**, 157–159.
34 N. Moazami, K. Fukamachi, M. Kobayashi, N. G. Smedira, K. J. Hoercher, A. Massiello, S. Lee, D. J. Horvath and R. C. Starling, *J. Heart Lung Transplant.*, 2013, **32**, 1–11.
35 A. Prinzing, U. Herold, A. Berkefeld, M. Krane, R. Lange and B. Voss, *J. Thorac. Dis.*, 2016, **8**, E660–E666.
36 M. H. Jung and F. Gustafsson, *J. Heart Lung Transplant.*, 2015, **34**, 489–496.
37 D. G. Jakovljevic, R. S. George, D. Nunan, G. Donovan, R. S. Bougard, M. H. Yacoub, E. J. Birks and D. A. Brodie, *Heart*, 2010, **96**, 1390–1395.
38 P. Brassard, A. S. Jensen, N. Nordsborg, F. Gustafsson, J. E. Moller, C. Hassager, S. Boesgaard, P. B. Hansen, P. S. Olsen, K. Sander, N. H. Secher and P. L. Madsen, *Circ.: Heart Failure*, 2011, **4**, 554–560.
39 K. Muthiah, D. Robson, R. Prichard, R. Walker, S. Gupta, A. M. Keogh, P. S. Macdonald, J. Woodard, E. Kotlyar, K. Dhital, E. Granger, P. Jansz, P. Spratt and C. S. Hayward, *J. Heart Lung Transplant.*, 2015, **34**, 522–529.
40 L. Fresiello, C. Gross and S. Jacobs, *Ann. Cardiothorac. Surg.*, 2021, **10**, 339–352.
41 A. S. Varshney, E. M. DeFilippis, J. A. Cowger, I. Netuka, S. P. Pinney and M. M. Givertz, *J. Am. Coll. Cardiol.*, 2022, **79**, 1092–1107.
42 D. McGiffin, *Heart, Lung Circ.*, 2016, **25**, e91–e92.
43 L. Harvey, C. T. Holley and R. John, *Ann. Cardiothorac. Surg.*, 2014, **3**, 475–479.
44 M. S. Mohamed, A. Shehadah, A. Hashem, S. Chand, J. Bapaye, A. Khalouf, D. Rai and S. Peter, *Am. J. Cardiol.*, 2023, **201**, 71–77.
45 G. Mawardi, T. M. Markman, R. Muslem, M. Sobhanian, M. Converse, H. B. Meadows, W. E. Uber, S. D. Russell, R. Rouf, B. Ramu, D. P. Judge, R. J. Tedford and B. A. Houston, *Heart, Lung Circ.*, 2020, **29**, 1241–1246.
46 M. Liebo, J. Newman, M. Yu, Z. Hussain, S. Malik, B. Lowes, C. Joyce, R. Zolty, H. I. Basha, A. Heroux, E. J. McGee, J. Y. Um and E. Raichlin, *ASAIO J.*, 2021, **67**, 324–331.
47 A. C. Lopilato, C. T. Doligalski and C. Caldeira, *Artif. Organs*, 2015, **39**, 939–944.
48 R. Bahuva, J. Giordano, S. Monahan, F. Dadi, A. Singh, H. Fichadiya, V. Hayagreev, U. Younus and A. Bahekar, *JACC Case Rep.*, 2025, **30**, 103961.
49 S. Schueler, C. T. Bowles, R. Hinkel, R. Wohlfarth, M. R. Schmid, S. Wildhirt, U. Stock, J. Fischer, J. Reiser and C. Kamla, *J. Thorac. Cardiovasc. Surg.*, 2023, **166**, 1119–1129. e1111.
50 T. Saygin Avsar, L. Jackson, P. Barton, S. Beese, O. O. Chidubem, S. Lim, D. Quinn, M. J. Price and D. J. Moore, *PharmacoEconomics Open*, 2025, **9**, 351–363.
51 J. Beca, T. Willcox and R. M. O. Hall, in *Cardiothoracic Critical Care*, ed. D. Sidebotham, A. McKee, M. Gillham and J. H. Levy, Butterworth-Heinemann, Philadelphia, 2007, pp. 342–364, DOI: 10.1016/b978-075067572-7.50025-4.
52 M. P. Peev and C. T. Salerno, in *Mechanical Circulatory Support*, ed. F. A. Arabía, Springer International Publishing, Cham, 2023, ch. 9-1, pp. 1–18, DOI: 10.1007/978-3-030-86172-8_9-1.
53 S. P. Chaudhry, A. D. DeVore, H. Vidula, M. Nassif, K. Mudy, E. Y. Birati, T. Gong, P. Atluri, D. Pham, B. Sun, A. Bansal and S. S. Najjar, *J. Am. Heart Assoc.*, 2022, **11**, e027251.
54 N. Hertz, PQDT-Global, 2025.
55 K. Kiyono, S. Tanabe, S. Hirano, T. Ii, Y. Nakagawa, K. Tan, E. Saitoh and Y. Otaka, *J. Clin. Med.*, 2024, **13**, 6616.
56 D. Kongahage, A. Ruhparwar and J. Foroughi, *Adv. Mater. Technol.*, 2021, 6.
57 S.-H. Sunwoo, S. I. Han, C. S. Park, J. H. Kim, J. S. Georgiou, S.-P. Lee, D.-H. Kim and T. Hyeon, *Nat. Rev. Bioeng.*, 2023, **2**, 8–24.
58 M. P. Hager, P. Ganguly and G. V. Letsou, *JACC Basic Transl. Sci.*, 2025, **10**, 101254.
59 I. Pirozzi, A. Kight, A. K. Han, M. R. Cutkosky and S. A. Dual, *Adv. Mater.*, 2024, **36**, e2210713.
60 C. Heim, N. Ebel, D. W. Schuberth, S. Werner, M. Kondruweit, R. Tandler and M. Weyand, *J. Heart Lung Transplant.*, 2019, **38**, S365–S366.

61 M. Sun, V. R. LaSala, C. Giuglaris, D. Blitzer, S. Jackman, S. Ustunel, K. Rajesh and D. Kalfa, *Bioeng. Transl. Med.*, 2025, **10**, e10706.
62 D. T. Nguyen and A. Z. Tumolo, *J. Am. Heart Assoc.*, 2019, **5**, 78–80.
63 E. T. Roche, M. A. Horvath, I. Wamala, A. Alazmani, S. E. Song, W. Whyte, Z. Machaidze, C. J. Payne, J. C. Weaver, G. Fishbein, J. Kuebler, N. V. Vasilyev, D. J. Mooney, F. A. Pigula and C. J. Walsh, *Sci. Transl. Med.*, 2017, **9**, 1–12.
64 J. C. Criscione, B. Leschinsky, W. C. Altman, E. C. Hord, C. M. Bolch and G. V. Letsou, *Rev. Cardiovasc. Med.*, 2022, 23.
65 E. C. Hord, C. M. Bolch, E. Tuzun, W. E. Cohn, B. Leschinsky and J. C. Criscione, *J. Cardiovasc. Transl. Res.*, 2019, **12**, 155–163.
66 G. Letsou, B. Leschinsky, W. Altman, C. Bolch, E. Hord and J. Criscione, *J. Heart Lung Transplant.*, 2023, **42**, S411–S412.
67 J. Kim, J. Lee, S. Song, S. H. Kang and A. K. Han, *Adv. Intell. Syst.*, 2025, **7**, 2500076.
68 M. A. Horvath, E. T. Roche, D. M. Vogt, D. J. Mooney, F. A. Pigula and C. J. Walsh, *Proc. ASME Int. Des. Eng. Tech. Conf. Comput. Inf. Eng. Conf.*, 2015, **V003T14A011**, DETC2015-47567.
69 Y. Wang, Z. Xie, H. Huang and X. Liang, *Smart Med.*, 2024, **3**, e20230045.
70 G. L. Anstadt and W. S. Blakemore, *Circ.*, 1965, 4–43.
71 M. Naveed, L. Han, G. J. Khan, S. Yasmeen, R. Mikrani, M. Abbas, L. Cunyu and Z. Xiaohui, *Biomed. Pharmacother.*, 2018, **102**, 41–54.
72 R. T. Kung and M. Rosenberg, *Ann. Thorac. Surg.*, 1999, **68**, 764–767.
73 C. J. Payne, I. Wamala, D. Bautista-Salinas, M. Saeed, D. Van Story, T. Thalhofer, M. A. Horvath, C. Abah, P. J. Del Nido, C. J. Walsh and N. V. Vasilyev, *Sci. Rob.*, 2017, **2**, eaan6736.
74 N. Kellaris, V. Gopaluni Venkata, G. M. Smith, S. K. Mitchell and C. Keplinger, *Sci. Rob.*, 2018, **3**, eaar3276.
75 C. S. Haines, M. D. Lima, N. Li, G. M. Spinks, J. Foroughi, J. D. Madden, S. H. Kim, S. Fang, M. Jung de Andrade, F. Goktepe, O. Goktepe, S. M. Mirvakili, S. Naficy, X. Lepro, J. Oh, M. E. Kozlov, S. J. Kim, X. Xu, B. J. Swedlove, G. G. Wallace and R. H. Baughman, *Science*, 2014, **343**, 868–872.
76 C. S. Haines, N. Li, G. M. Spinks, A. E. Aliev, J. Di and R. H. Baughman, *Proc. Natl. Acad. Sci. U. S. A.*, 2016, 113, 11709–11716.
77 S. Naficy, G. M. Spinks and R. H. Baughman, in *Bio-inspired Polymers*, The Royal Society of Chemistry, 2016, pp. 429–459, DOI: 10.1039/9781782626664-00429.
78 T. Martinez, J. Chavanne, A. Walter, Y. Civet and Y. Perriard, *Smart Mater. Struct.*, 2021, **30**, 105024.
79 A. Benouhiba, A. Walter, S. Ekroll Jahren, F. Clavica, D. Obrist, Y. Civet and Y. Perriard, *Adv. Eng. Mater.*, 2025, 2501234.
80 T. Martinez, S. E. Jahren, A. Walter, J. Chavanne, F. Clavica, L. Ferrari, P. P. Heinisch, D. Casoni, A. Haeberlin, M. M. Luedi, D. Obrist, T. Carrel, Y. Civet and Y. Perriard, *Bioeng. Transl. Med.*, 2023, **8**, e10396.
81 S. E. Jahren, T. Martinez, A. Walter, L. Ferrari, F. Clavica, D. Obrist, Y. Civet and Y. Perriard, *J. Biomech.*, 2023, **159**, 111777.
82 J. Mau, S. Menzie, Y. Huang, M. Ward and S. Hunyor, *Thorac. Cardiovasc. Surg.*, 2011, **142**, 209–215.
83 A. K. Chin, P. Neuzil and G. V. Noriega, in *Extracorporeal Membrane Oxygenation – Evolving Innovations*, IntechOpen, 2026, DOI: 10.5772/intechopen.1014733.
84 H. Cui, C. Liu, T. Esworthy, Y. Huang, Z. X. Yu, X. Zhou, H. San, S. J. Lee, S. Y. Hann, M. Boehm, M. Mohiuddin, J. P. Fisher and L. G. Zhang, *Sci. Adv.*, 2020, 6.
85 H. Schotola, S. T. Sossalla, A. Renner, J. Gummert, B. C. Danner, P. Schott and K. Toischer, *ESC Heart Fail.*, 2017, **4**, 468–478.
86 S. E. Jahren, T. Martinez, A. Walter, F. Clavica, P. P. Heinisch, E. Buffle, M. M. Luedi, J. Horer, D. Obrist, T. Carrel, Y. Civet and Y. Perriard, *Int. Cardiovasc. Thorac. Surg.*, 2024, **38**, ivae027.
87 J. Zhao, R. Ghannam, K. O. Htet, Y. Liu, M. K. Law, V. A. L. Roy, B. Michel, M. A. Imran and H. Heidari, *Adv. Healthcare Mater.*, 2020, **9**, 2000779.
88 R. H. Baughman, *Synth. Met.*, 1996, **78**, 339–353.
89 B. Guo, L. Glavas and A.-C. Albertsson, *Prog. Polym. Sci.*, 2013, **38**, 1263–1286.
90 J. K. Ponniah, H. Chen, O. Adetiba, R. Verduzco and J. G. Jacot, *J. Mater. Chem. B*, 2016, **4**, 7350–7362.
91 Z. Wan, W. Chen, C. Liu, Y. Liu and C. Dong, *J. Colloid Interface Sci.*, 2015, **443**, 115–124.
92 P. Shokrollahi, Y. Omidi, L. X. Cubeddu and H. Omidian, *J. Biomed. Mater. Res., Part B*, 2023, **111**, 1979–1995.
93 T. Khan, G. Vadivel, K. Ayyasamy, G. Murugesan and T. A. Sebaey, *Polymers*, 2025, **17**, 620.
94 A. Ghodsizad, A. Ruhparwar, V. Bordel, E. Mirsaidighazi, H. M. Klein, M. M. Koerner, M. Karck and A. El-Banayosy, *Cardiovasc. Ther.*, 2013, **31**, 323–334.
95 A. Ruhparwar, P. Piontek, M. Ungerer, A. Ghodsizad, S. Partovi, J. Foroughi, G. Szabo, M. Farag, M. Karck, G. M. Spinks and S. J. Kim, *Artif. Organs*, 2014, **38**, 1034–1039.
96 S. Kim, C. Laschi and B. Trimmer, *Trends Biotechnol.*, 2013, **31**, 287–294.
97 M. Shahinpoor and K. J. Kim, *Smart Mater. Struct.*, 2001, **10**, 819–833.
98 M. Hosseinipour and M. Elahinia, *Smart Mater. Struct.*, 2013, **22**, 125017.
99 M. S. Kim, J. K. Heo, H. Rodrigue, H. T. Lee, S. Pané, M. W. Han and S. H. Ahn, *Adv. Mater.*, 2023, **35**, 2208517.
100 H. Holman, M. N. Kavarana and T. K. Rajab, *Artif. Organs*, 2021, **45**, 454–463.
101 P.-D. K. Kalogerakos, I. A. Hassoulas and V. S. Ladopoulos, *Hellenic J. Cardiol.*, 2010, **51**, 301–309.
102 Y. Shiraishi, T. Yambe, K. Sekine, N. Masumoto, J. Nagatoshi, S. Itoh, Y. Saijo, Q. Wang, H. Liu, S. Nitta, S. Konno, D. Ogawa, P. Olegario, M. Yoshizawa, A. Tanaka,

F. Sato, Y. Park, M. Uematsu, M. Higa, Y. Hori, T. Fujimoto, K. Tabayashi, H. Sasada, M. Umezu and D. Homma, *Annu. Int. Conf. IEEE Eng. Med. Biol. Soc., IEEE*, 2005, **7**, 406–408.
103 S. Chitsaz, J. F. Wenk, L. Ge, A. Wisneski, A. Mookhoek, M. B. Ratcliffe, J. M. Guccione and E. E. Tseng, *Ann. Thorac. Surg.*, 2013, **95**, 148–154.
104 J. Mu, M. Jung de Andrade, S. Fang, X. Wang, E. Gao, N. Li, S. H. Kim, H. Wang, C. Hou, Q. Zhang, M. Zhu, D. Qian, H. Lu, D. Kongahage, S. Talebian, J. Foroughi, G. Spinks, H. Kim, T. H. Ware, H. J. Sim, D. Y. Lee, Y. Jang, S. J. Kim and R. H. Baughman, *Science*, 2019, **365**, 150–155.
105 S. E. Bakarich, R. Gorkin, R. Gately, S. Naficy, M. in het Panhuis and G. M. Spinks, *Addit. Manuf.*, 2017, **14**, 24–30.
106 M. Jessup, *J. Heart Lung Transplant.*, 2000, **19**, S68–72.
107 J. Davies, E. Nicotra, K. Zhu, C. C. Nguyen, B. Sharma, A. Ji, P. T. Phan, J. Wan, P. Pruscino and H. Truong, *Adv. Sci.*, 2026, e16667.
108 L. Rosalia, C. Ozturk, D. Goswami, J. Bonnemain, S. X. Wang, B. Bonner, J. C. Weaver, R. Puri, S. Kapadia and C. T. Nguyen, *Sci. Rob.*, 2023, **8**, eade2184.
109 L. Rosalia, C. Ozturk, S. X. Wang, D. Quevedo-Moreno, M. Y. Saeed, A. Mauskapf and E. T. Roche, *Adv. Funct. Mater.*, 2024, **34**, 2310085.
110 C. Park, M. Singh, M. Y. Saeed, C. T. Nguyen and E. T. Roche, *Device*, 2024, 2.
111 M. Bakouri, *IET Syst. Biol.*, 2018, **12**, 68–72.
112 Y. Wu, P. Allaire, G. Tao, H. Wood, D. Olsen and C. Tribble, *Artif. Organs*, 2003, **27**, 926–930.
113 H. Liu and S. Liu, *Biomed. Signal Process. Control*, 2025, **100**, 107020.
114 J. Cysyk, R. Newswanger, E. Popjes, W. Pae, C. S. Jhun, J. Izer, W. Weiss and G. Rosenberg, *ASAIO J.*, 2019, **65**, 318–323.
115 M. Fetanat, M. Stevens, C. Hayward and N. H. Lovell, *IEEE Trans. Biomed. Eng.*, 2019, **67**, 1167–1175.
116 Y. Leng and R. Sun, *Adv. Healthcare Mater.*, 2025, e2500860.
117 J. Lin, R. Fu, X. Zhong, P. Yu, G. Tan, W. Li, H. Zhang, Y. Li, L. Zhou and C. Ning, *Cell Rep. Phys. Sci.*, 2021, **2**, 100541.
118 H. A. Owida, *Int. J. Biomater.*, 2022, **2022**, 8312564.
119 A. Weymann, J. Foroughi, R. Vardanyan, P. P. Punjabi, B. Schmack, S. Aloko, G. M. Spinks, C. H. Wang, A. Arjomandi Rad and A. Ruhparwar, *Adv. Mater.*, 2023, **35**, e2207390.
120 E. T. Roche, M. A. Horvath, A. Alazmani, K. C. Galloway, N. V. Vasilyev, D. J. Mooney and F. A. Pigula, *Proc. ASME Int. Des. Eng. Tech. Conf. Comput. Inf. Eng. Conf.*, 2015, DETC2015-47566.
121 S. Nakatani, *J. Cardiovasc. Ultrasound*, 2011, **19**, 1–6.
122 S. Mohsen and J. K. Kwang.
123 S. C. Obiajulu, E. T. Roche, F. A. Pigula and C. J. Walsh, *Proc. ASME Int. Des. Eng. Tech. Conf. Comput. Inf. Eng. Conf.*, 2013, **V06AT07A009**, DETC2013-13004.
124 R. A. J. Carrington, Y. Huang, O. Kawaguchi, T. Yuasa, K. Shirota, D. Martin and S. N. Hunyor, *Ann. Thorac. Surg.*, 2003, **75**, 190–196.
125 A. Loforte, G. Gliozzi, C. Mariani, G. G. Cavalli, S. Martin-Suarez and D. Pacini, *Cardiovasc. Diagn. Ther.*, 2020, **11**, 277–291.
126 J. S. Hanke, G. Dogan, M. Shrestha, A. Haverich and J. D. Schmitto, *JTCVS Open*, 2021, **8**, 28–32.
127 S. Wildhirt, A. Ruhparwar, S. Schueler, U. Stock, J. S. Hanke, J. D. Schmitto, H. Pauli, J. Karsten, F. Gustafsson and B. Schmack, *JACC Basic Transl. Sci.*, 2025, **10**, 267–269.
128 M. A. Horvath, C. E. Varela, E. B. Dolan, W. Whyte, D. S. Monahan, C. J. Payne, I. A. Wamala, N. V. Vasilyev, F. A. Pigula, D. J. Mooney, C. J. Walsh, G. P. Duffy and E. T. Roche, *Ann. Biomed. Eng.*, 2018, **46**, 1534–1547.
129 D. A. Kass, K. L. Baughman, P. H. Pak, P. W. Cho, H. R. Levin, T. J. Gardner, H. R. Halperin, J. E. Tsitlik and M. A. Acker, *Circulation*, 1995, **91**, 2314–2318.
130 H. Suga and K. Sagawa, *Circ. Res.*, 1974, **35**, 117–126.
131 J. Aboulhosn and J. S. Child, *Circulation*, 2006, **114**, 2412–2422.
132 M. N. Kavarana, H. M. Loree, 2nd, R. B. Stewart, M. T. Milbocker, R. L. Hannan, G. M. Pantalos and R. T. Kung, *J. Cardiovasc. Dis. Diagn.*, 2013, **1**, 1000105.
133 M. A. Horvath, I. Wamala, E. Rytkin, E. Doyle, C. J. Payne, T. Thalhofer, I. Berra, A. Solovyeva, M. Saeed, S. Hendren, E. T. Roche, P. J. Del Nido, C. J. Walsh and N. V. Vasilyev, *Ann. Biomed. Eng.*, 2017, **45**, 2222–2233.
134 M. P. Anstadt, R. L. Bartlett, J. P. Malone, G. R. Brown, S. Martin, D. J. Nolan, K. H. Oberheu and G. L. Anstadt, *Chest*, 1991, **100**, 86–92.
135 R. L. Bartlett, N. J. Stewart, Jr., J. Raymond, G. L. Anstadt and S. D. Martin, *Ann. Emerg. Med.*, 1984, **13**, 773–777.
136 A. Weymann, J. Foroughi, R. Vardanyan, P. P. Punjabi, B. Schmack, S. Aloko, G. M. Spinks, C.-H. Wang, A. A. Rad and A. Ruhparwar, *Adv. Mater.*, 2022, 2207390.
137 S. A. Dual, J. Cowger, E. Roche and A. Nayak, *J. Card. Failure*, 2024, **30**, 596–609.
138 P. Rothemund, N. Kellaris, S. K. Mitchell, E. Acome and C. Keplinger, *Adv. Mater.*, 2021, **33**, e2003375.
139 M. D. Lima, M. W. Hussain, G. M. Spinks, S. Naficy, D. Hagenasr, J. S. Bykova, D. Tolly and R. H. Baughman, *Small*, 2015, **11**, 3113–3118.
140 B. Fang, Y. Xiao, Z. Xu, D. Chang, B. Wang, W. Gao and C. Gao, *Mater. Horiz.*, 2019, **6**, 1207–1214.
141 Y. Sun, Y. Wang, C. Hua, Y. Ge, S. Hou, Y. Shang and A. Cao, *Carbon*, 2018, **132**, 394–400.
142 S. H. Kim, C. H. Kwon, K. Park, T. J. Mun, X. Lepro, R. H. Baughman, G. M. Spinks and S. J. Kim, *Sci. Rep.*, 2016, **6**, 23016.
143 T. Jia, Y. Wang, Y. Dou, Y. Li, M. Jung de Andrade, R. Wang, S. Fang, J. Li, Z. Yu, R. Qiao, Z. Liu, Y. Cheng, Y. Su, M. Minary-Jolandan, R. H. Baughman, D. Qian and Z. Liu, *Adv. Funct. Mater.*, 2019, **29**, 1808241.
144 K. Matsumoto, N. Sakikawa and T. Miyata, *Nat. Commun.*, 2018, **9**, 2315.
145 Z. Jiang, B. B. A. Abbasi, S. Aloko, F. Mokhtari and G. M. Spinks, *Adv. Mater.*, 2023, **35**, e2210419.
146 C. Li, J. Li, H. Duan and X. Yi, *Adv. Funct. Mater.*, 2025, e14063.
147 A. Ferrari, C. Giampietro, B. Bachmann, L. Bernardi, D. Bezuidenhhout, P. Ermanni, R. Hopf, S. Kitz, G. Kress, C. Loosli, V. Marina, M. Meboldt, G. Pellegrini, D. Poulikakos, M. Rebholz, M. Schmid Daners, T. Schmidt, C. Starck, G. Stefopoulos, S. Sundermann, B. Thamsen,

P. Zilla, E. Potapov, V. Falk and E. Mazza, *Ann. Biomed. Eng.*, 2021, **49**, 716–731.

148 Y. Pya, J. Maly, M. Bekbossynova, R. Salov, S. Schueler, B. Meyns, Y. Kassif, M. Massetti, M. Zilbershlag and I. Netuka, *J. Heart Lung Transplant.*, 2019, **38**, 339–343.

149 E. T. Roche, M. A. Horvath, I. Wamala, A. Alazmani, S.-E. Song, W. Whyte, Z. Machaidze, C. J. Payne, J. C. Weaver, G. Fishbein, J. Kuebler, N. V. Vasilyev, D. J. Mooney, F. A. Pigula and C. J. Walsh, *Sci. Transl. Med.*, 2017, **9**, eaaf3925.